*Mathematical Problems in Engineering*
Volume 3, pp. 413–477
Reprints available directly from the publisher
Photocopying permitted by license only



# The *V*-Transform: A Tool for Analysis of Control Systems Robustness with respect to Disturbance Model Uncertainty

D.E. DAVISON, P.T. KABAMBA and S.M. MEERKOV*

*Department of Electrical Engineering and Computer Science, University of Michigan, Ann Arbor, MI 48109, USA*

*(Received 19 February 1997)*

This work is motivated by the need for tools for the analysis of disturbance model uncertainty in feedback control systems. Such tools are developed in this paper for the case where the disturbance is modeled as the output of a first-order filter which is driven by white noise and whose bandwidth, $\omega_d$, and gain, $K$, are uncertain. An analytical expression for the steady-state output variance as a function of $\omega_d$ is derived: This function is referred to as a $V$-transform, and is denoted by $V(G)(\omega_d)$, where $G(s)$ is the closed-loop transfer function from disturbance to output. Properties of $V$-transforms are investigated and the notions of *disturbance gain margin* and *disturbance bandwidth margin*, both measures of robustness with respect to disturbance model uncertainty, are introduced. Using these new tools, it is shown that there is a fundamental robustness performance limitation if the plant has nonminimum-phase zeros, but no such limitation in the minimum-phase case.

*Keywords:* Control system; Disturbance rejection; Performance limitation; Robustness analysis; Uncertainty; Variance

* Corresponding author. Tel.: +1 (313) 763-6349. Fax: +1 (313) 763-8041. E-mail: smm@eecs.umich.edu.

# 1 INTRODUCTION

## 1.1 Motivation

The robustness of control system performance with respect to *plant model* uncertainty has been studied in the control community for decades (e.g., see [1–5] and the references therein). In contrast, robustness of performance with respect to *disturbance model* uncertainty has received far less attention. Typically, it is *assumed* that the disturbance belongs to a given class of signals (e.g., signals with bounded amplitude, or signals with bounded energy, or stochastic processes with given power spectral density), and a controller is designed to accommodate in a desirable manner disturbances generated by such a model. The question of what happens if the actual disturbance violates the assumption is, typically, ignored. Consequently, if the disturbance does indeed violate the assumption, unsatisfactory performance may result. An example of such a case is provided in a recent National Transportation Safety Board report which cites an incident on January 7, 1997, in which a jetliner cruising over the Atlantic Ocean encountered unexpected turbulence, resulting in six injured persons (one serious) and minor aircraft damage [6]. Our interpretation of the root cause of this incident is that the encountered turbulence was of a different nature than the turbulence model used in the autopilot design and evaluation.

The main goal of this paper is to introduce measures of performance robustness with respect to disturbance model uncertainty and to use these measures for control systems analysis. "Performance" here refers to the disturbance rejection ability of a controller. The particular issues addressed include the following:

- How does disturbance rejection performance vary with changes in the disturbance model?
- How can disturbance rejection robustness be quantified?
- Are there fundamental limits on disturbance rejection robustness?

The significance of these questions can be illustrated as follows.

*Example 1.1* Consider the design of an airplane autopilot for the regulation of the airplane's vertical velocity in the presence of wind. A very simple model of the airplane, wind, and controller is provided in Fig. 1. The plant is the airplane, modeled as a point mass subject to

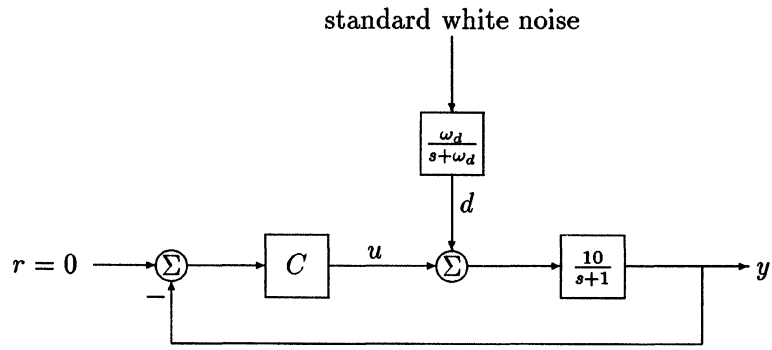


FIGURE 1 Model used in Example 1.1.

atmospheric drag. The plant input is the sum of the net vertical force applied by the plane's lifting surfaces ($u$) and the force due to the wind ($d$). The plant output is the plane's vertical velocity ($y$). The wind disturbance is modeled as the output of a first-order low-pass filter that is driven by standard white noise, that is, Gaussian white noise with unit power spectral density. Suppose that experimental measurements indicate that a "typical" wind disturbance can be described by such a model with a bandwidth of 1 rad/s. In this case the disturbance filter bandwidth, $\omega_d$, is set to 1 and is regarded as a fixed parameter.

The design objective is to find a controller that decreases the effect of wind disturbances on the output $y$ by a factor of at least ten when compared with open-loop performance. Assume that wind attenuation is measured by the steady-state variance of $y$; a calculation indicates that the open-loop steady-state variance is 25, so this specification corresponds to a desired closed-loop steady-state variance of no more than 2.5. Two controllers that satisfy this specification are

$$C_1(s) = \frac{0.5(s+2)}{s} \quad \text{and} \quad C_2(s) = 0.86.$$

The gains have been chosen so that the controllers satisfy the design specification equally well: in both cases, the steady-state variance of $y$ is 0.49. Therefore, with respect to *nominal* disturbance rejection, the controllers are equally good.

Suppose now that the wind bandwidth is actually 20% higher than modeled, that is, $\omega_d = 1.2$ rad/s. The same controllers now result in

significantly different disturbance rejection behavior: The output steady-state variance with $C_1$ in place is 0.64, whereas the output steady-state variance with $C_2$ in place is 0.58. In other words, a 20% increase in wind bandwidth results in a 31% degradation in performance for $C_1$, but only a 18% degradation in performance for $C_2$. This shows that the disturbance robustness properties of $C_1$ and $C_2$ are significantly different. Other calculations confirm this conclusion. For instance, with controller $C_1$ in place, the disturbance bandwidth can increase to 3.7 rad/s before the performance specification is violated. For $C_2$, the equivalent figure is much higher, at 8.9 rad/s. Therefore, with respect to *robust* disturbance rejection, controller $C_2$ is superior to controller $C_1$. More complete analysis of the disturbance rejection robustness of $C_1$ and $C_2$ is carried out when this example is revisited in Section 6.

## 1.2 Problem Formulation

The single-input single-output system under consideration is shown in Fig. 2. Transfer function $C$ is the controller and transfer functions $P_1$, $P_2$, and $P_3$ comprise the plant. Signal $r$ is the command reference signal, $u$ is the control signal, $y$ is the output, and $d$ is the disturbance, modeled as the output of the filter $KF$, where $K > 0$ is an uncertain parameter

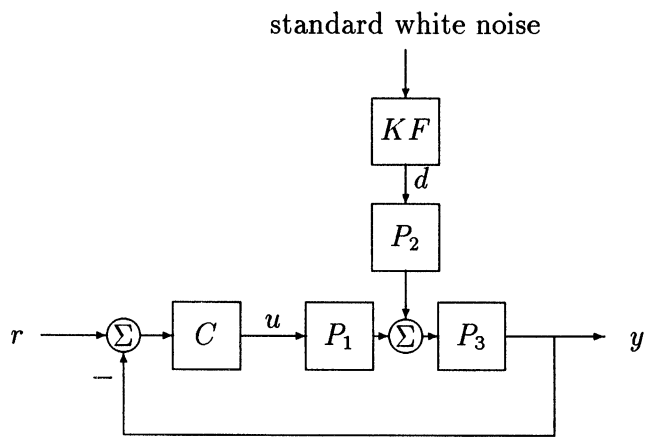


FIGURE 2 System model.

(with nominal value $K^*$) and $F$ is the filter

$$F(s) \triangleq \frac{\omega_d}{s+\omega_d}, \tag{1}$$

where $\omega_d > 0$ is an uncertain parameter (with nominal value $\omega_d^*$). Parameter $\omega_d$ can be interpreted as the disturbance bandwidth, and parameter $K$ determines the low-frequency power spectral density (PSD). Indeed, the PSD of $d$ is

$$S_d(\omega) = |KF(j\omega)|^2 = \frac{K^2\omega_d^2}{\omega^2+\omega_d^2}.$$

The performance measure which will be used to evaluate the disturbance rejection ability of a given controller is the *steady-state variance* of $y$. This performance measure is useful in many engineering applications. For example, there is a relationship between the variance of vertical acceleration and the comfort of passengers in airplanes [7,8] and in automobiles [9–12]. As another example, variance is closely related to the notions of *probability of exceedence* and *residence time*, concepts that are important in several fields of study, including aiming control (which includes telescope pointing, missile terminal guidance, robot arm pointing, etc.) [13–18], aircraft gust load analysis [19,20], and ship stabilization in waves [21]. It also turns out that steady-state variance (hereafter just called variance) is easy to compute. Indeed, denote the closed-loop transfer function from $d$ to $y$ in Fig. 2 by $G$:

$$G(s) = \frac{P_3(s)P_2(s)}{1+P_3(s)P_1(s)C(s)}. \tag{2}$$

Then it is a standard result (e.g., see [22]) that, if $GF$ is stable and strictly proper,[1] then the variance of $y$ is

$$\frac{1}{2\pi}\int_{-\infty}^{\infty} |G(j\omega)KF(j\omega)|^2 \, d\omega = K^2\|GF\|_2^2, \tag{3}$$

where $\|\cdot\|_2$ is the $\mathcal{H}_2$-norm.

[1] A rational transfer function is *proper* if the degree of the numerator is no larger than the degree of the denominator; it is *strictly proper* if the degree of the numerator is less than the degree of the denominator; it is *biproper* if the degrees are equal; it is *improper* if it is not proper.

The assumptions associated with Fig. 2 are collected below. Assumptions 2 and 3 were previously introduced, Assumptions 1 and 4 are made for simplicity, and Assumptions 5 and 6 are introduced, respectively, to ensure well-posedness and to ensure the existence of an internally-stabilizing controller:

**Assumption 1** Transfer functions $P_1$, $P_2$, $P_3$, and $C$ are rational and proper.

**Assumption 2** Disturbance $d$ is the output of the filter $KF$ (where $F(s) = \omega_d/(s+\omega_d)$), which, in turn, is driven by standard white noise. The disturbance is not measurable for control purposes.

**Assumption 3** The output variance is used as a measure of the influence that the disturbance has on the closed-loop system.

**Assumption 4** There is no sensor noise.

**Assumption 5** Transfer function $P_3P_1$ is strictly proper.

**Assumption 6** There are no unstable pole-zero cancelations in $P_3P_1$, and $P_2$ is stable.

The problem is to address, under the above assumptions, the three issues stated earlier. Specifically:

- investigate how the variance of $y$ behaves as a function of $\omega_d$ and $K$,
- quantify disturbance rejection robustness, and
- determine if there are limitations on the achievable performance robustness.

*Remark 1.1* The results in this paper are easily adapted to other forms of the disturbance filter $F$. For example, if the filter is of the form

$$f(\omega_d)\frac{\omega_d}{s+\omega_d}, \tag{4}$$

where $f$ is a known function of $\omega_d$, then the output variance is simply scaled by the factor $f^2(\omega_d)$. One case that has been found to be useful is $f(\omega_d) = \sqrt{2/\omega_d}$: In this specific case, it can be shown (using, for example, Theorem 4.1 given below) that the variance of $d$ is $K^2$ (i.e., it is independent of $\omega_d$).

## 1.3 Literature Review

The literature review has three components. First, several examples of models representing disturbances of practical importance are given, and the associated model uncertainty is discussed. Second, a brief review of how disturbance model uncertainty is handled in the control literature is given. Lastly, since it is possible to rearrange the system in Fig. 2 so that the disturbance model becomes part of the plant, the relevant literature on *plant model* uncertainty is summarized.

### *1.3.1 Instances of Uncertain Disturbance Models*

Three instances of random disturbances which have uncertain statistics have been researched, namely, wind turbulence models, water wave models, and road roughness models.

*Wind Turbulence Models* Wind is obviously a significant disturbance in aircraft control problems, but it also can be significant in automobile, ship, and telescope pointing systems, for example. For simplicity, the discussion here is limited to models of turbulence at altitudes greater than several thousand feet; see [7], [23], or [24] (and the references therein) for discussion on low-altitude turbulence. Similarly, the discussion is limited to *continuous* turbulence models; see, for example, [7], [19], or [24] for discrete models, that is, models used to represent single large gusts such as those due to buildings, aircraft wakes, or shear layers.

According to [24], experimental data indicates that continuous turbulence takes the form of individual patches. In each patch the turbulence is essentially random, homogeneous (i.e., the statistical properties are the same at every point) and isotropic (i.e., the statistical properties are independent of axis translation, rotation, and reflection). Furthermore, it is usually assumed that the turbulence is stationary and that the turbulence patches are "frozen" in space. These turbulence properties are, of course, idealizations; see [7] for a discussion of deficiencies with the homogeneous and isotropic assumptions and see, for example, [25] for a discussion of nonstationary turbulence models.

It is common to decompose the turbulence velocity vector into three components, corresponding to the longitudinal, lateral, and vertical

directions. Since the three components are handled in essentially the same way and since Ref. [24] indicates that the vertical component is the most important turbulence component at high altitude flight, only the vertical component is considered here. Experimental and theoretical results indicate that wind turbulence spectra roll off as $\omega^{-5/3}$; the so-called Von Kármán spectrum satisfies this property and has become a standard turbulence model. The Von Kármán spectrum for the vertical turbulence velocity component is [20,24,26–28]:

$$S(\omega) = \sigma_w^2 \frac{L}{V} \frac{1 + \frac{8}{3}(1.339L\omega/V)^2}{[1 + (1.339L\omega/V)^2]^{11/6}}. \tag{5}$$

In this expression, $\sigma_w^2$ is the turbulence variance, $L$ is the so-called turbulence scale, and $V$ is the aircraft airspeed. There is usually not much uncertainty associated with $V$; however, both $\sigma_w$ and $L$ vary with altitude and the characteristics of the turbulence, and, consequently, there is uncertainty as to what the "correct" values are. This uncertainty arises since the parameters must be determined experimentally, and all measurements have errors, but, more significantly, the turbulence characteristics at a given altitude are not invariant. Indeed, in practice $\sigma_w$ is often treated as a random variable whose distribution is dependent on altitude [7,8,19,20]. It is also common to assign a particular value of $\sigma_w$ to each altitude under different degrees of turbulence: Table 9.62 in [24] plots $\sigma_w$ versus altitude in clear air turbulence (with typical values between 4.5 ft/s and 6.5 ft/s in the altitude range 1000–30 000 ft); the same reference advising using 21 ft/s in thunderstorm turbulence for altitudes up to 40 000 ft. In contrast to the treatment of $\sigma_w$, uncertainty in $L$ does not appear to be explicitly considered, even though uncertainty in $L$ is recognized. Indeed, for the Von Kármán model it is recommended that, in both clear air turbulence (for altitudes greater than 2500 ft) and thunderstorm turbulence, $L$ be set to 2500 ft [24], but values of $L$ from as small as 490 ft to as large as 4900 ft have been proposed [7]. As more evidence of the uncertainty in $L$, Ref. [27] goes so far as to assign a probability distribution to $L$; the mean value is in the range 500–700 ft. Moreover, Ref. [20] mentions that $L$ probably varies considerably from patch to patch, and, more significantly, "more often than not, the PSD of a

particular patch of turbulence does not fit the (Von Kármán model) very well for *any* value of $L$." In a discussion about accidents due to turbulence and wind shear, the author of [7] acknowledges that "even something as basic as the 'correct' value of the integral scale of atmospheric turbulence eludes us."

*Water Wave Models* Water waves act as disturbances on every surface-traveling ship, but are also important for submarines traveling near the surface and for fixed sea platforms (e.g., oil drilling rigs). For simplicity, the discussion here is limited to fully developed ocean waves. Furthermore, the effects of swell and wave spreading are also ignored, even though both can be important [29].

Despite appearances at the shoreline, ocean waves are chaotic in the open ocean. Reference [30] includes a variety of photographs showing the wide range of wave systems that occur. Indeed, it was thought early on that modeling such wave systems was not possible, but, to improve the success of amphibious operations in World War II, the first scientific theory of water wave forecasting was developed in 1942–1947 [31,32]. The theory was found to be inadequate, and a new theory based on stochastic processes was developed in the following two decades. An often cited spectrum for open ocean wave amplitudes is the Bretschneider or ITTC (International Towing Tank Conference) 2-parameter spectrum [29]:

$$S(\omega) = \frac{A}{\omega^5} \exp(-B/\omega^4), \tag{6}$$

where

$$A = 487.3\pi \frac{\bar{H}_1^2}{T_0^4} \quad \text{and} \quad B = \frac{1949}{T_0^4}. \tag{7}$$

Here, $T_0$ is the modal period of the spectrum and $\bar{H}_1$ is the characteristic wave height as defined in [29]. (For our purposes, the precise definitions of these quantities are not important.) The variance of the amplitude is completely determined by $\bar{H}_1$; for fixed $\bar{H}_1$, the spectrum resembles a single hump whose peak value and peak frequency vary with $T_0$.

The literature has several variations of spectrum (6). For example, Refs. [33,35] refer to (6) with $A$ and $B$ defined in terms of a single

parameter. A generalization of (6) is also mentioned in [33]:

$$S(\omega) = \frac{A}{\omega^m} \exp(-B/\omega^4).$$

Here, $m$ is an integer to be chosen based on "the experience and judgment of engineers" and the constants $A$ and $B$ are now complicated expressions, omitted for brevity. Finally, Ref. [33] cites a paper which describes a detailed six-parameter ocean wave spectrum.

The spectra mentioned above apply to stationary objects in the water. For moving objects (e.g., ships), it is necessary to modify the spectrum, or, equivalently, to modify the frequency $\omega$. As shown in [29,34], the frequency encountered by a ship moving at speed $V$ and angle of encounter $\mu$ is

$$\omega_e = \omega - \frac{\omega^2 V}{g} \cos(\mu),$$

assuming deep water. Both references describe how to determine the wave spectra in terms of $\omega_e$.

Even under the simplifying assumptions above, there is considerable uncertainty in the wave spectra:

- Since several different spectra have been proposed in the literature, and there is not a consensus as to which one is "correct," it is reasonable to conclude that the statistics of ocean waves are variable. Therefore, there is uncertainty as to whether any particular spectrum (computed based on data from a particular location and a particular time) is suitable for another location or another time.
- The determination of the spectrum parameters (e.g., $A$ and $B$) is ultimately based on experimental data, and all experimental measurements involve uncertainty. Measuring wave characteristics is particularly difficult [29,36]. There is also measurement error associated with finding $V$ and $\mu$ to determine the encountered spectrum.

Perhaps even more significant than the above sources of uncertainty, the underlying assumptions add uncertainty:

- In the presence of swell, the wave spectrum can change dramatically. Reference [33] states that there are essentially no models of swell because observational data is so scarce.

- Wave spreading has been ignored above (as is often done in the literature) even though almost all open ocean waves do, in fact, exhibit wave spreading (i.e., they are "short-crested") [29]. Unlike swell, it is at least possible to (partially) compensate for wave spreading by appropriate modification of the spectrum [29,33], but the study of short-crested waves is a current research area.
- The spectra change significantly in shallow water or in limited-fetch (coastal) areas. References [29,33,34] discuss these issues.
- Nonlinear and nonstationary effects have been ignored. However, there is evidence that nonlinear effects play a significant role [33,36].

*Road Roughness Models* The roughness of roads is important because it affects ride quality, rate of road deterioration, and vehicle operating cost [11,37]. It is argued in [38] that road roughness is also a major variable in the economic evaluation of highway systems and [39] uses cost data to conclude that "reducing vehicle operating costs by even a fraction of a percent will do more to reduce the total transportation costs than anything that can be done to reduce the cost of constructing or maintaining pavements." To reduce vehicle operating costs, the roads can be made smoother or the vehicles can be designed to better handle the roughness. In the latter case, modifying suspension systems (passively or actively) is the most obvious way of improving vehicle tolerance to rough roads and, simultaneously, improving ride comfort. The authors of [40] argue that a good road roughness model is needed for theoretical analysis and design purposes, and they conclude that the major source of error in predicting ride quality is an inadequate description of road roughness.

Several assumptions about road roughness are usually made for simplicity. Generally, models are based on continuous road roughness, that is, they exclude occasional large irregularities such as potholes. It is also usually assumed that the road surface is two-dimensional (i.e., the left and right side of the car experience the same bumps); Ref. [41] considers a full three-dimensional model and shows that typical road surfaces can indeed be considered to be realizations of homogeneous and isotropic two-dimensional Gaussian random processes. Usually other types of forces (e.g., braking or turning forces, wind gusts) are ignored when considering road roughness; Ref. [9] states that road roughness is the most relevant type of force for ride studies, so ignoring these other forces is reasonable.

Several references indicate that it is important to have an accurate road profile model. For instance, the author of [10] states that the "dynamical interaction between the road and vehicle changes drastically depending on road surface and vehicle velocity." As another example, the authors of [40] show by comparing experimental and theoretical data that "the major source of error in predicting ride quality will come from an inadequate description of roadway roughness." (They are referring in particular to the inadequacies of spectrum (8), given below.)

There are several road roughness spectra in the literature. The following spectra are for road *displacement*:

- The simplest, and probably the most commonly used, spectrum has the form

$$S(\omega) = \frac{cV}{\omega^2}, \tag{8}$$

  where $c$ is a constant called the *road roughness coefficient*, *roughness parameter*, or *roughness constant*, and where $V$ is the vehicle's speed. The value of $c$ varies by several orders of magnitude depending on the road conditions [9,40]. The authors of [40] carried out experimental studies and concluded that model (8) is inadequate for road roughness spectra unless the frequency range of concern is very limited. Other presentations of experimental data (e.g., [41,42]) also show that the constant $-2$ slope is not very accurate for some road surfaces.
- A generalization of (8) often mentioned (e.g., see [9]) is

$$S(\omega) = \frac{cV^{n-1}}{\omega^n}, \tag{9}$$

  where $n > 0$ is a second parameter usually close to 2. The author of [9] states that (9) (and therefore, (8)) is not always a good approximation; he includes several experimental spectra as evidence.
- An even more general form of (8) mentioned in [40,41,43,44] is

$$S(\omega) = \begin{cases} (\alpha/V)(\omega_0/\omega)^{n_1} & \text{if } \omega < \omega_0, \\ (\alpha/V)(\omega_0/\omega)^{n_2} & \text{if } \omega \geq \omega_0, \end{cases} \tag{10}$$

where $\alpha$, $n_1$, and $n_2$ depend on the properties of the road; the particular values vary significantly with road conditions [41,43,44]. Generally, $\omega_0$ is set to $V$ for all road surfaces [41], i.e., the corresponding "spatial frequency" is assumed to be 1 rad/m.

- A third generalization of (8) has the form [43]

$$S(\omega) = \frac{cV}{\omega^2}\left(1 + \frac{\Omega_0^2 V^2}{\omega^2}\right), \tag{11}$$

where $c$ is the road roughness coefficient and $\Omega_0$ is the cutoff frequency. The reference suggests using $\Omega_0 = 0.16(2\pi)$ rad/m for bituminous roads and $\Omega_0 = 0.07(2\pi)$ rad/m for portland cement concrete roads.

- Reference [45] uses the following spectrum:

$$S(\omega) = \sigma^2 \frac{2aV}{\omega^2 + a^2 V^2}, \tag{12}$$

where $\sigma^2$ is the variance of the road irregularities and $a$ is a coefficient dependent on the type of road surface.

- In many of the references, small peaks are evident in the experimentally determined spectra, but none of the spectra given above include such peaks. (These peaks are especially significant for terrain road surfaces, as opposed to smooth roads.) The spectrum given in [10] does include these peaks, but is, consequently, fairly complicated. It is given by

$$S(\omega) = \sigma_1^2 \frac{2\alpha_1 V}{\omega^2 + \alpha_1^2 V^2} + \sigma_2^2 \frac{2\alpha_2 V(\omega^2 + \alpha_2^2 V^2 + \beta^2 V^2)}{(\omega^2 + \alpha_2^2 V^2 - \beta^2 V^2)^2 + 4\alpha_2^2 \beta^2 V^4}, \tag{13}$$

where $\alpha_1$, $\alpha_2$, $\beta$, $\sigma_1$, and $\sigma_2$ are tabulated in [10] according to the surface type (asphalt, paved, or dirt).

Based on the collection of models given above, it can be concluded that road roughness models vary greatly. Therefore, no single fixed spectrum is suitable for all road surfaces. Moreover, even for a specific type of surface (e.g., asphalt), the models differ, especially at low frequencies.

It follows that, even for a fixed surface type, the road roughness spectra are uncertain. Note that, conceptually, road roughness is very similar to wind turbulence (under the frozen patch assumption). Also note that road roughness is an issue for not only vehicles, but also for aircraft [46] and, slightly modified, for trains [47,48].

### 1.3.2 Disturbance Model Uncertainty in the Control Literature

In the control literature, it is common to model random disturbances as filtered white noise where the filter is a rational transfer function. The disturbance filters used are often very simple. For example, it is common to use a simple gain, i.e., to model the disturbance as white noise. Although white noise is a purely mathematical artifact, this approach can often be justified because the designer is not using the disturbance filter to model a true disturbance, but, rather, as a "tuning knob" for the design process. In cases where an attempt is made to model a real disturbance, first-order filters are often used; such simple filters are used instead of more detailed models since the PSD of the disturbance is "rarely known precisely" [49]. However, there are cases where second or higher-order filters are used. For example, it is common to approximate the irrational Von Kármán turbulence spectrum (5) by the so-called Dryden spectrum [24,28]

$$S(\omega) = \sigma_w^2 \frac{L}{V} \frac{1 + 3(L\omega/V)^2}{[1 + (L\omega/V)^2]^2},$$

which can be generated by passing white noise through a second-order filter. Other higher-order rational approximations to the Von Kármán spectrum exist [20]. Examples of high-order rational approximations to ocean wave spectra are found in [50,51].

It appears that *uncertainty* in disturbance (or noise) filters is not considered in the control literature very often. However, there are several relevant threads of research:

- In [52] it is recognized that disturbance model uncertainty is a significant issue when dealing with the problem of *state estimation* under process and measurement noise. The authors study cases where the PSD of one of the noise sources is uncertain and where the other is white noise with known PSD. In the scalar-state case,

the authors also mention the *spectral band noise model*, in which the PSD of the fixed-power noise signal is assumed to lie between known lower and upper bounds. However, in the multivariable-state case, they constrain themselves to white noise with uncertain PSD matrices. The approach of the paper is to optimize the worst-case mean-square error by forming a minimax optimization problem. Earlier state estimation papers of a similar nature include [53–56].

- There are several studies of the LQG problem under disturbance and noise model uncertainty [57–60]. However, in all cases, the noise sources are assumed to be white with uncertainty only in the magnitude of the PSD.
- In [61–64], problems where the covariance sequence of the disturbance belongs to a prespecified set are considered. For both control and filtering problems, the author develops minimax design procedures, although the tools used are completely different than the minimax schemes used in the previously cited references.
- The use of *bounding filters* is an alternative strategy for treating estimation problems with uncertain plant state-space matrices and uncertain noise statistics [65–67]. The idea is to design for a spectrum that bounds the possible noise spectra. As discussed in [54], this simple approach can be useful, but it also can lead to conservative designs and, moreover, it is not applicable if the noise spectra cannot be bounded. Reference [68] uses a bounding approach in an optimal control problem.
- One of the original motivating factors of $\mathcal{H}_\infty$-theory was the observation that quadratic-norm methods generally ignore uncertainty in disturbance power spectra [69,70]. $\mathcal{H}_\infty$-theory accounts for disturbance power spectrum uncertainty in a minimax sense; however, the method can be very conservative since, effectively, no information other than the disturbance power is used.
- Several papers that deal with the notion of uncertain disturbance models in a *nonstochastic* framework have been found. For example, Ref. [71] considers the effect of nonperiodic disturbances on repetitive control systems, that is, systems where it is assumed that the disturbances are periodic.

Most of the above papers take a minimax approach to design, that is, the authors essentially assume conditions that ensure the existence of a

worst-case disturbance, then they design for that disturbance. Alternatively, an *adaptive* approach is possible (e.g., see [72,73]). The authors of [73] discuss in fairly general terms how parameter uncertainty (in both the plant and disturbance models) can be accommodated by having the controller adapt to the changing parameters. Paper [74] cites several references that discuss the advantages and disadvantages of minimax and adaptive schemes. Since the focus of this paper is on robust disturbance rejection, adaptive disturbance rejection will not be considered further.

### 1.3.3 Treating Disturbance Model Uncertainty as Plant Model Uncertainty

In the feedback structure of Fig. 2, there is a clear distinction between plant and disturbance models, and, therefore, a clear distinction between plant and disturbance model uncertainty. A recent trend is to combine the plant and disturbance models (along with any performance weights) into a single *generalized plant*. This is the approach taken in $\mathcal{H}_2$, $\mathcal{H}_\infty$, and $\mu$ synthesis techniques (e.g., see [3,5,75]). The question arises as to whether the vast literature on $\mathcal{H}_2$, $\mathcal{H}_\infty$, and $\mu$ techniques applies to our problem. Since the uncertainties in question are parametric and the performance measure is computed by a $\mathcal{H}_2$-norm, only the $\mathcal{H}_2$-literature that deals with parametric uncertainty in the generalized plant is relevant. Because the $\mathcal{H}_2$-problem can be posed as an LQG problem [76], this includes any LQG literature that deals with parametric plant uncertainty. This literature can be roughly classified according to the method of treatment of the uncertain parameters, and includes the random variable approach (e.g., [77–79]), the minimax approach (e.g., [79,80]), the artificial multiplicative noise approach [81], the "parameter robust LQG" approach [82,83], and the "guaranteed cost control" approach (e.g., [84–86]).

Intuitively, the problem of parameter uncertainty in the disturbance model is much simpler than the problem of parameter uncertainty in the (nongeneralized) plant model. Indeed, it is impossible for any variation of the disturbance filter to affect any loop characteristic, including stability. (This is not true if adaptive disturbance rejection is used or if the disturbance is measurable, however.) Thus, one expects that treatment of parameter uncertainty in the disturbance model alone

should be easier than the treatment of parameter uncertainty in the generalized plant, and, therefore, there should be no need to invoke the rather complicated mathematical machinery required for the latter. Because of this, and since it is not immediately evident that any of the methods described in the above references can solve our problem,[2] none of the material presented in this paper relies on the above references.

### 1.4 Paper Outline

In Section 2 we introduce the basic tool that is used to investigate how the variance of $y$ behaves as a function of the disturbance bandwidth, $\omega_d$. We call this tool the $V$-transform. In Section 3, quantitative measures of disturbance rejection robustness are defined in terms of $V$-transforms; they are similar to phase margin and gain margin, the classical measures of *stability* robustness. Section 4 then investigates mathematical properties of $V$-transforms. For example, it is shown that the variance of $y$ is a rational function of $\omega_d$ whose "state-space realization" has the same poles as those of the closed-loop system. Other properties studied include the continuity, convexity, monotonicity, and asymptotic behavior of the $V$-transform. In Section 5, we consider the problem of designing a controller to achieve a given level of disturbance rejection robustness, as measured by the $V$-transform. It is shown that there is a limitation on disturbance rejection robustness in the nonminimum-phase case, but no such limitation in the minimum-phase case. Finally, Section 6 presents two simple examples, and Section 7 concludes the paper. All proofs are given in the Appendix.

## 2 THE $V$-TRANSFORM

Denote by $\mathcal{RH}_\infty$ and $\mathcal{RH}_2$ the set of stable rational transfer functions that are, respectively, proper and strictly proper. (Every transfer function in $\mathcal{RH}_\infty$ has finite $\mathcal{H}_\infty$-norm, and every transfer function in

[2] For example, no references could be found that address the basic issue of determining how the performance index varies with the uncertain parameters.

$\mathcal{RH}_2$ has finite $\mathcal{H}_2$-norm [5].) Also introduce the following notation: for scalar $q$ (real or complex) and matrices $A, B, C, D$ of appropriate dimensions, define

$$\left[\begin{array}{c|c} A & B \\ \hline C & D \end{array}\right](q) \triangleq D + C(qI - A)^{-1}B.$$

Lastly, denote by $\mathcal{R}_+$ the set of nonnegative real numbers. Then the $V$-transform is defined as follows:

DEFINITION 2.1 Let $G$ be an element of $\mathcal{RH}_\infty$ and let $F$ be the filter $\omega_d/(s+\omega_d)$. The *V-transform of G*, denoted $V(G)$, is the function mapping $\mathcal{R}_+$ into itself defined by

$$V(G)(\omega_d) = \|GF\|_2^2.$$

In other words, $V(G)(\omega_d)$ is the variance of $y$, explicitly as a function of $\omega_d$, when $K=1$. For general $K$, the output variance is $V(KG)(\omega_d) = K^2V(G)(\omega_d)$. This relationship is shown pictorially in Fig. 3.

The "$V$" in $V$-transform stands for "variance"; this is appropriate since $V(G)(\omega_d)$ has an interpretation as variance for each $\omega_d$. The word "transform" is also appropriate since $V(G)$ transforms $G$, a function of $s$, into a function of $\omega_d$. Indeed, $V(G)$ is formed by integrating $|G(j\omega)|^2$, weighted by a rational kernel:

$$V(G)(\omega_d) = \|GF\|_2^2 = \frac{1}{\pi}\int_0^\infty |G(j\omega)|^2 \frac{\omega_d^2}{\omega^2 + \omega_d^2}\, d\omega.$$

This has a similar structure to other transforms, such as the Laplace transform (except the Laplace transform is based on a *transcendental* kernel). The mathematical properties of $V$-transforms are explored in Section 4.

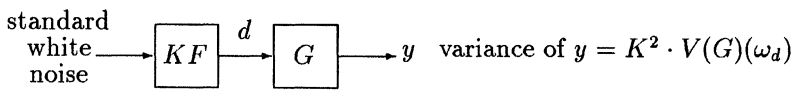


FIGURE 3 Relationship between $G$ and $V(G)$.

Note that $V(G)$ is a *global* transformation of $G$ in the sense that the computation of $V(G)(\omega_d)$ requires knowledge of $|G(j\omega)|$ for all $\omega \in \mathcal{R}_+$. It is therefore not surprising that it can be difficult to make conclusions about the robustness of closed-loop disturbance rejection by examining only the Bode plot of $G$, as the following example illustrates.

*Example 2.1* Consider the system in Fig. 2 with

$$K = 1, \quad P_1(s) = 1, \quad P_2(s) = 1, \quad P_3(s) = \frac{1}{(s+1)^3}.$$

It can be verified that the proportional controller $C(s) = k$ internally stabilizes the system for $-1 < k < 8$. Consider three particular controllers:

$$C_1(s) = 1, \quad C_2(s) = 4, \quad C_3(s) = 7.25.$$

The corresponding closed-loop transfer functions from $d$ to $y$ are

$$G_1(s) = \frac{1}{s^3 + 3s^2 + 3s + 2}, \quad G_2(s) = \frac{1}{s^3 + 3s^2 + 3s + 5},$$

$$G_3(s) = \frac{1}{s^3 + 3s^2 + 3s + 8.25}.$$

The Bode magnitude plots of $G_1$, $G_2$, and $G_3$ are shown in Fig. 4. (The phase plots are not included since the variance is completely determined by the magnitude of $G$.) The frequency axis has been partitioned into four regions, denoted R1, R2, R3, and R4 in the figure. The relative ability of the controllers to reject *particular frequency components* of disturbance $d$ depends on which region the frequency component is in. Table I summarizes the results. Observe that controller $C_3$ is the best of the three controllers at rejecting frequencies in regions R1 and R2 (corresponding to frequencies less than 1.3 rad/s); hence, a reasonable hypothesis is that for low $\omega_d$ (i.e., when $d$ has low bandwidth), controller $C_3$ results in the lowest variance. Unfortunately, it is difficult to predict anything more than this based solely on the Bode plots.

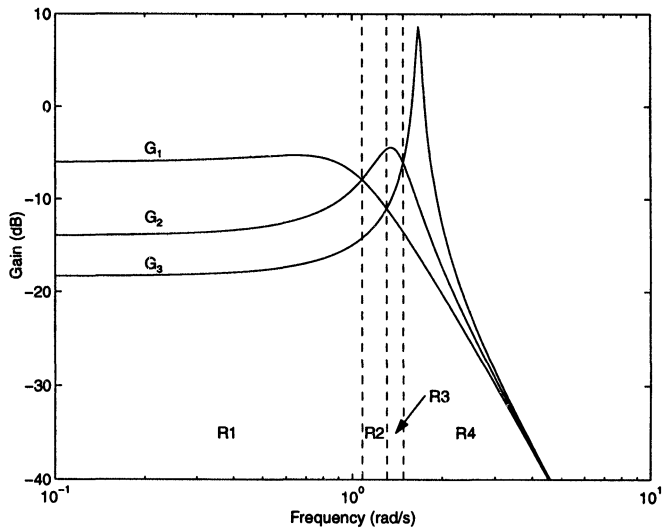


FIGURE 4 Bode magnitude plots of $G_1$, $G_2$, and $G_3$ in Example 2.1. The relative ability of the controllers to reject a particular frequency component of the disturbance depends on which region the frequency is in.

TABLE I Comparison of the relative abilities of the three controllers in Example 2.1 to reject a single frequency component of disturbance $d$

| | *Frequency region R1* | *Frequency region R2* | *Frequency region R3* | *Frequency region R4* |
|---|---|---|---|---|
| Best controller | $C_3$ | $C_3$ | $C_1$ | $C_1$ |
| Middle controller | $C_2$ | $C_1$ | $C_3$ | $C_2$ |
| Worst controller | $C_1$ | $C_2$ | $C_2$ | $C_3$ |

To determine precisely how the controllers compare with respect to $\omega_d$, Fig. 5 shows $V(G_1)$, $V(G_2)$, and $V(G_3)$;[3] for clarity the horizontal scale is logarithmic. The relative performance of the three controllers differs in each of the regions marked R1′, R2′, and R3′ in the figure. Table II summarizes the results, and Fig. 6 shows regions R1′, R2′, and R3′ superimposed on the Bode magnitude plots from Fig. 4. As hypothesized earlier, controller $C_3$ is the best of the three controllers for low $\omega_d$, but only in region R1′, corresponding to $\omega_d < 0.23$ rad/s. For

[3] All $V$-transforms are computed using Theorem 4.1.

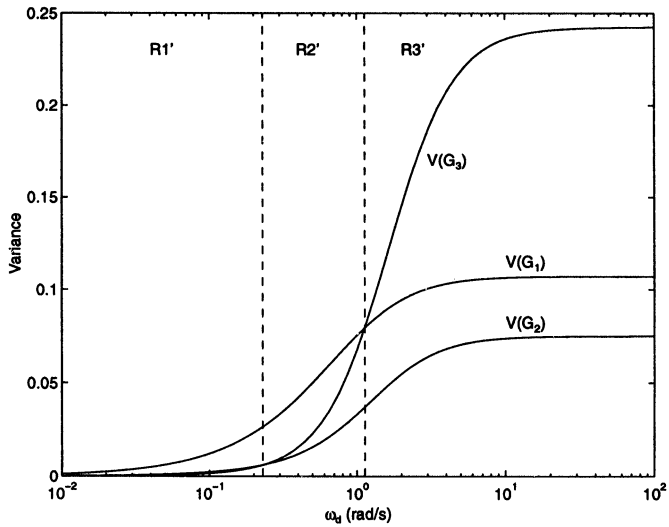


FIGURE 5 $V$-transforms of $G_1$, $G_2$, and $G_3$ in Example 2.1. The relativex performance of the three controllers at rejecting disturbances depends on which region the disturbance bandwidth is in.

TABLE II Comparison of the relative abilities of the three controllers in Example 2.1 to reject disturbances of bandwidth $\omega_d$

| | $\omega_d$ *region* $R1'$ | $\omega_d$ *region* $R2'$ | $\omega_d$ *region* $R3'$ |
|---|---|---|---|
| Best controller | $C_3$ | $C_2$ | $C_2$ |
| Middle controller | $C_2$ | $C_3$ | $C_1$ |
| Worst controller | $C_1$ | $C_1$ | $C_3$ |

$\omega_d > 0.23$ rad/s, controller $C_2$ is the best. Controller $C_1$ is never the best controller from the viewpoint of output variance. It is claimed that, without explicit use of the $V$-transform, such conclusions could not be drawn.

This section is concluded with some observations:

- Example 2.1 shows that the examination of the Bode plot of $G$ may be insufficient to draw conclusions about the disturbance rejection robustness capabilities of a controller. Since the loop gain $L \triangleq P_3P_1C$ includes no information about $P_2$ or the location of where the disturbance is injected, it is reasonable to expect that

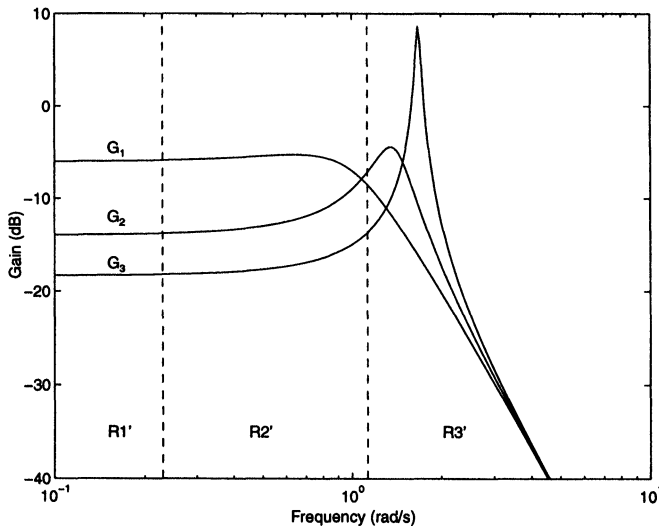


FIGURE 6 Bode magnitude plots of $G_1$, $G_2$, and $G_3$ in Example 2.1. The relative performance of the controllers at rejecting disturbances depends on which region the disturbance bandwidth is in. In particular, controller $C_3$ is the best at rejecting disturbances if the disturbance bandwidth is in region R1′, and controller $C_2$ is the best otherwise.

examination of the Bode plot of $L$ will be even less useful than the examination of the Bode plot of $G$.

- A key issue in comparing $V$-transforms is whether or not the $V$-transforms cross (since the controller which is superior on one side of the crossing is necessarily inferior on the other side). It is easy to show that if the Bode magnitude plots of $G_1$ and $G_2$ (corresponding to two different controllers) do not cross, then $V(G_1)$ and $V(G_2)$ do not cross either; however, if the Bode magnitude plots of $G_1$ and $G_2$ do cross, then it cannot be concluded whether or not $V(G_1)$ and $V(G_2)$ cross.
- The "$G$" in the expression $V(G)$ need not arise from (2); indeed, $V(G)$ is well defined and meaningful for any stable transfer function $G$. In particular, the variance of any signal (or filtered version thereof) in Fig. 2, not just that of $y$, can be expressed in terms of $V$-transforms. Similarly, the robustness margins defined in the next section apply to any signal. It is only for simplicity that the focus of the paper rests only on the variance of signal $y$.

## 3 ROBUSTNESS MARGINS

Let $\gamma > 0$ denote the threshold of the variance of $y$ that determines acceptable performance. Assume that

$$V(K^*G)(\omega_d^*) < \gamma,$$

that is, nominal performance is achieved. It is natural to ask how much $K$ and $\omega_d$ can vary from their nominal values before (if ever) performance becomes unacceptable. The following scalars are measures of robustness with respect to these types of variations:

- Define the *disturbance gain margin* ($\mathrm{DGM}_\gamma$) to be the largest increase in $K$ (as a multiple of its nominal value) that can be tolerated until performance becomes unacceptable:

$$\mathrm{DGM}_\gamma \triangleq \sqrt{\frac{\gamma}{V(K^*G)(\omega_d^*)}}.$$

- Define the *disturbance bandwidth margin* ($\mathrm{DBM}_\gamma$) as the largest increase in $\omega_d$ (as a multiple of its nominal value) that can be tolerated until performance becomes unacceptable:

$$\mathrm{DBM}_\gamma \triangleq \sup\left\{\frac{\bar{\omega}_d}{\omega_d^*} : \bar{\omega}_d \geq \omega_d^* \text{ and } \forall \omega_d \in [\omega_d^*, \bar{\omega}_d],\ V(K^*G)(\omega_d) \leq \gamma\right\}.$$

(For convenience define the supremum of an unbounded set of positive real numbers to be infinity.)

The concepts of disturbance gain margin and disturbance bandwidth margin appear to be new. The following example illustrates that $\mathrm{DGM}_\gamma$ and $\mathrm{DBM}_\gamma$ are easily determined graphically; the example also shows that $\mathrm{DGM}_\gamma$ and $\mathrm{DBM}_\gamma$ are independent of several classical measures of merit.

*Example 3.1* Consider the system in Fig. 2 with

$$P_1(s) = 1,\ P_2(s) = 1,\ P_3(s) = 1/s,\ K^* = 1,\ \omega_d^* = 2\,\mathrm{rad/s},\ \gamma = 0.4,$$

and consider the following two internally stabilizing controllers:

$$C_1(s) = \frac{s/100 + 1}{s/10 + 1} \quad \text{and} \quad C_2(s) = \frac{(s/15 + 1)^2}{(s/100 + 1)^2}.$$

The controllers have very similar gain margins (both infinite), phase margins (85° and 96°, respectively), gain cross-over frequencies (0.995 rad/s and 1.004 rad/s, respectively), and low-frequency reference tracking characteristics (see Fig. 7). Indeed, the loop gain Bode plots are essentially the same up to 1 rad/s (see Fig. 8). It follows that neither controller is superior than the other at rejection of low-frequency components of the disturbance, and one might therefore conjecture that, as measured by variance, the rejection properties of the two controllers are essentially the same. However, inspection of the $V$-transforms (see Fig. 9) reveals that the robustness properties with respect to uncertainty in $K$ and $\omega_d$ are actually quite different. Indeed, the previously defined robustness margins are, for $C_1$,

$$\text{DGM}_\gamma = \sqrt{\frac{0.4}{0.356}} = 1.06 \quad \text{and} \quad \text{DBM}_\gamma = \frac{2.90}{2.0} = 1.45,$$

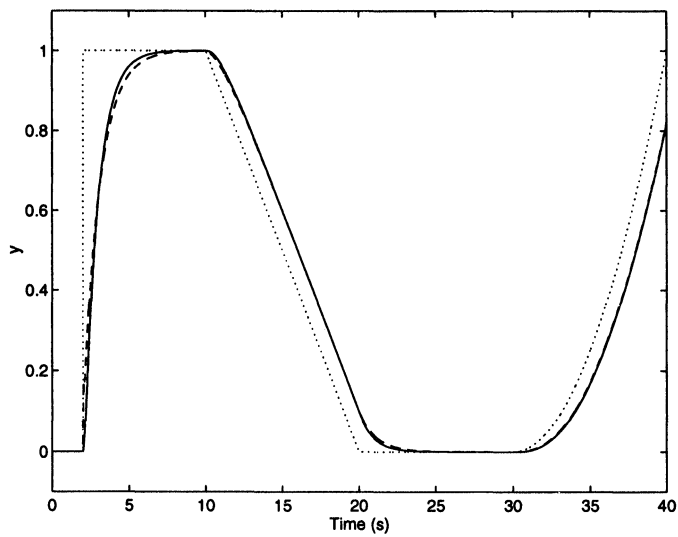


FIGURE 7 Tracking behavior for $C_1$ (solid) and $C_2$ (dashed) in Example 3.1. The dotted curve is the reference signal.

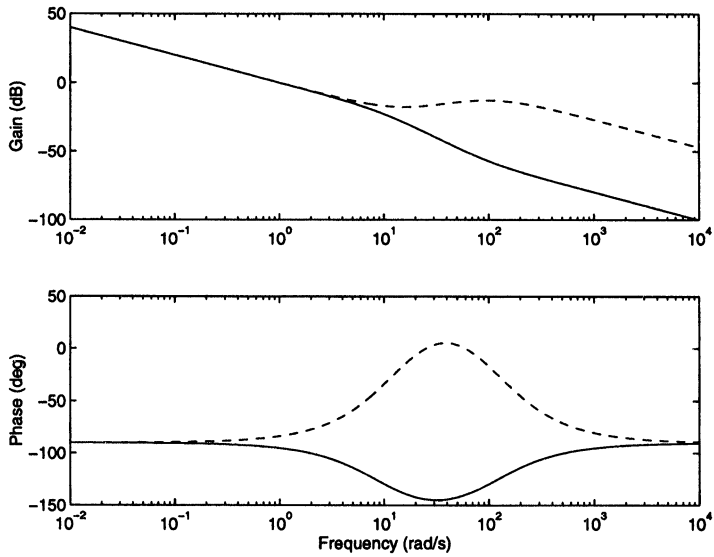


FIGURE 8 Bode plots of the loop gain for $C_1$ (solid) and $C_2$ (dashed) in Example 3.1.

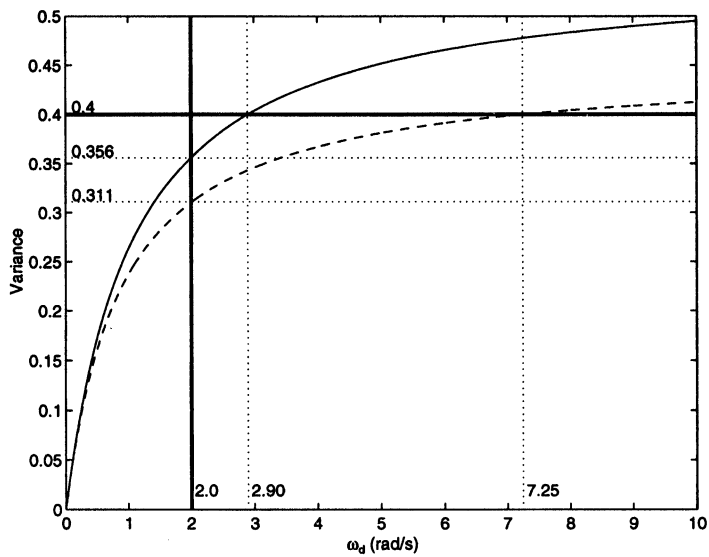


FIGURE 9 $V$-transforms for $C_1$ (solid) and $C_2$ (dashed) in Example 3.1.

and, for $C_2$,

$$\mathrm{DGM}_\gamma = \sqrt{\frac{0.4}{0.311}} = 1.13 \quad \text{and} \quad \mathrm{DBM}_\gamma = \frac{7.25}{2.0} = 3.63.$$

(The numbers in these equations are all taken from Fig. 9.) The conclusion is that $C_2$ has superior disturbance rejection robustness than that of $C_1$.

*Remark 3.1* It is well known that stability gain and phase margins do not always capture the system's true stability robustness. (See [5] for examples of contrived systems with good gain and phase margins, but poor stability robustness.) Similarly, the disturbance gain and bandwidth margins are not always a good measure of a system's disturbance rejection robustness. Examples can be constructed where $\mathrm{DBM}_\gamma$ is infinite, yet a slight perturbation in the $V$-transform causes $\mathrm{DBM}_\gamma$ to become finite. Similarly, it is possible that $\mathrm{DGM}_\gamma$ changes significantly (although it is always finite) by a slight system perturbation. In each case, the examples are contrived, and it has been found that, typically, $\mathrm{DGM}_\gamma$ and $\mathrm{DBM}_\gamma$ appear to be good robustness measures.

## 4 $V$-TRANSFORM PROPERTIES

Two types of properties of $V(G)(\omega_\mathrm{d})$ are described, namely, properties that arise by treating $\omega_\mathrm{d}$ as an independent variable (for fixed $G$), and those that arise by treating $G$ as an independent variable.

### 4.1 Properties of $V(G)(\omega_\mathrm{d})$ as a Function of $\omega_\mathrm{d}$

#### *4.1.1 V-Transform Realizations*

The theorem in this subsection states that $V(G)(\omega_\mathrm{d})$ is a *rational* function of $\omega_\mathrm{d}$, and it presents two realizations of $V(G)$ in terms of a realization of $G$. The following lemma, used in the proof of the theorem, gives a standard way to compute $\mathcal{H}_2$-norms [5]:

LEMMA 4.1 *Given $M \in \mathcal{RH}_2$ with realization*

$$\left[\begin{array}{c|c} \check{A} & \check{B} \\ \hline \check{C} & 0 \end{array}\right](s),$$

*let* $\check{L}$ *denote the observability Grammian of* $(\check{C}, \check{A})$, *that is,* $\check{L}$ *is the unique solution of the Lyapunov equation* $\check{A}^{\mathrm{T}}\check{L} + \check{L}\check{A} + \check{C}^{\mathrm{T}}\check{C} = 0$. *Then* $\|M\|_2^2 = \check{B}^{\mathrm{T}}\check{L}\check{B}$.

Note that solving the Lyapunov equation for $\check{L}$ is a standard linear computation, easily performed, for example, by MATLAB.

THEOREM 4.1 *Given* $G \in \mathcal{RH}_\infty$ *with realization*

$$\left[\begin{array}{c|c} A & B \\ \hline C & D \end{array}\right](s),$$

*let* $L_o$ *be the observability Grammian of* $(C, A)$. *Define*

$$\hat{A} = \begin{bmatrix} A^{-1} & 0 \\ 0 & 0 \end{bmatrix}, \quad \hat{B} = \begin{bmatrix} A^{-1}B \\ \frac{1}{2}D^2 \end{bmatrix}, \quad \hat{C} = \begin{bmatrix} -(B^{\mathrm{T}}L_o + DC) & 1 \end{bmatrix},$$

$$\bar{A} = A, \quad \bar{B} = B, \quad \bar{C} = (B^{\mathrm{T}}L_o + DC)A, \quad \bar{D} = (B^{\mathrm{T}}L_o + DC)B.$$

*Then two realizations of* $V(G)$ *are*

$$V(G)(\omega_d) = \left[\begin{array}{c|c} \hat{A} & \hat{B} \\ \hline \hat{C} & 0 \end{array}\right]\left(\frac{1}{\omega_d}\right) \tag{14}$$

*and*

$$V(G)(\omega_d) = \left[\begin{array}{c|c} \bar{A} & \bar{B} \\ \hline \bar{C} & \bar{D} \end{array}\right](\omega_d) + \frac{1}{2}\omega_d D^2. \tag{15}$$

COROLLARY 4.1 *If* $D = 0$ *in Theorem* 4.1, *that is, if* $G$ *is strictly proper, then realizations* (14) *and* (15) *simplify to*

$$\left[\begin{array}{c|c} A^{-1} & A^{-1}B \\ \hline -B^{\mathrm{T}}L_o & 0 \end{array}\right]\left(\frac{1}{\omega_d}\right) \quad \textit{and} \quad \left[\begin{array}{c|c} A & B \\ \hline B^{\mathrm{T}}L_oA & B^{\mathrm{T}}L_oB \end{array}\right](\omega_d).$$

*Remark 4.1* If realization (15) is interpreted as a dynamical system (in $\omega_d$ instead of $s$), then the "poles" of $V(G)$ are seen to be the same as the poles of $G$. Why the dynamics of $G$ and the "dynamics" of $V(G)$ coincide is not clear. Furthermore, it is not clear how the "zeros" of $V(G)$ are related to $G$, or even what it means to interpret (15) as a dynamical system.

*Remark 4.2* The fact that $V(G)$ is *rational* in $\omega_d$ also follows from [87], where it is shown that the square of the $\mathcal{H}_2$-norm of

$$\left[\begin{array}{c|c} A(q) & B(q) \\ \hline C(q) & 0 \end{array}\right](s)$$

is rational if $A(q)$, $B(q)$, and $C(q)$ are affine functions of $q$. (The fact that the state-space matrices of $G(s)F(s)$ are affine in $\omega_d$ is apparent from Eq. (34) in the Appendix.)

### 4.1.2 Analyticity of $V(G)$

It is not unexpected that $V(G)(\omega_d)$ is an analytic function of $\omega_d$:

THEOREM 4.2 *For all* $G \in \mathcal{RH}_\infty$, $V(G)$ *is an analytic function of* $\omega_d \in \mathcal{R}_+$. *If*

$$\left[\begin{array}{c|c} A & B \\ \hline C & D \end{array}\right](s)$$

*is a realization of* $G$ *and if* $\bar{A}$, $\bar{B}$, *and* $\bar{C}$ *are defined as in Theorem* 4.1, *then*

$$\frac{d}{d\omega_d} V(G)(\omega_d) = -\bar{C}(\omega_d I - \bar{A})^{-2}\bar{B} + \frac{1}{2}D^2,$$

*and, for all integers* $m \geq 2$,

$$\frac{d^m}{d\omega_d^m} V(G)(\omega_d) = (-1)^m m!\bar{C}(\omega_d I - \bar{A})^{-(m+1)}\bar{B}.$$

### 4.1.3 Initial and Final Values

THEOREM 4.3 *For all* $G \in \mathcal{RH}_\infty$, $V(G)$ *satisfies the following*:

- $V(G)(0) = 0$.
- $dV(G)(0)/d\omega_d = G(0)^2/2$.
- *If* $G$ *is not identically zero then* $V(G)$ *is a strictly increasing function of* $\omega_d \in \mathcal{R}_+$.
- *Let*

$$\left[\begin{array}{c|c} A & B \\ \hline C & D \end{array}\right](s)$$

*be a realization of $G$, and let $L_o$ be the corresponding observability Grammian. Then, as $\omega_d \to \infty$, $V(G)(\omega_d)$ approaches*

$$B^T L_o B + DCB + \tfrac{1}{2}\omega_d D^2. \tag{16}$$

Theorem 4.3 has a natural interpretation in terms of variance. Recall that $V(G)(\omega_d)$ is the variance of the output of the filter $GF$ when $GF$ is driven by standard white noise. The first property in Theorem 4.3 simply says that the output variance is zero when the filter $F$ has zero bandwidth, an obvious result. The second result states that, as $\omega_d$ is increased from zero, the rate of increase of variance is proportional to the square of the DC gain of $G$. In other words, for very small $\omega_d$, the higher the DC gain of $G$, the more sensitive the output variance is to changes in $\omega_d$. The third property states that, as $\omega_d$ increases, the output variance increases; this is expected since increasing $\omega_d$ corresponds to increasing the bandwidth of $F$. The last property in Theorem 4.3 is best considered in two cases: First, if $G$ is strictly proper, i.e., $D = 0$, then Theorem 4.3 indicates that $V(G)(\omega_d) \to B^T L_o B = \|G\|_2^2$. This is expected since, as $\omega_d \to \infty$, $F$ tends to a unity gain filter, so the noise is filtered only by $G$. On the other hand, if $G$ is biproper, i.e., $D \neq 0$, then Theorem 4.3 indicates that $V(G)(\omega_d)$ is unbounded, and that it approaches the asymptote given in (16). Since $G$ is biproper, it can be decomposed into the parallel connection of a low-pass filter (i.e., $C(sI - A)^{-1}B$) and a nonzero constant gain (i.e., $D$). The noise that is processed by the low-pass filter makes a bounded contribution to the output variance, but the noise that is "filtered" by the constant gain makes a contribution to the output variance that is proportional to $\omega_d$.

### 4.1.4 Invertibility

The above results immediately lead to the following:

THEOREM 4.4 *For every $G \in \mathcal{RH}_\infty$, the inverse function $[V(G)]^{-1}$ is well defined. If $G \in \mathcal{RH}_2$, then the domain of $[V(G)]^{-1}$ is $[0, \|G\|_2^2]$; otherwise, the domain is $[0, \infty)$.*

Note that it is generally not possible to give a closed-form expression for $[V(G)]^{-1}$ since the required computation involves finding the roots of a polynomial whose order equals the number of poles of $G$.

*Remark 4.3* An equivalent definition of $\mathrm{DBM}_\gamma$ (see Section 3) is

$$\mathrm{DBM}_\gamma = \begin{cases} [V(G)]^{-1}(\gamma)/\omega_d^* & \text{if } G \in \mathcal{RH}_\infty - \mathcal{RH}_2 \text{ OR,} \\ & \text{if } G \in \mathcal{RH}_2 \text{ and } \|G\|_2^2 > \gamma, \\ \infty & \text{if } G \in \mathcal{RH}_2 \text{ and } \|G\|_2^2 \leq \gamma. \end{cases}$$

## 4.2 Properties of $V(G)(\omega_d)$ as a Function of $G$

### 4.2.1 Scaling

A simple result is that the $V$-transform is homogeneous of degree two:

THEOREM 4.5 *For all $G \in \mathcal{RH}_\infty$ and for all $\alpha \in \mathcal{R}$, $V(\alpha G) = \alpha^2 V(G)$.*

*Remark 4.4* If $F$ has the form of (4), then it follows from Theorem 4.5 that the output variance, as a function of $\omega_d$, is $f^2(\omega_d) \cdot V(G)(\omega_d)$. Theorem 4.1 can still be applied to give an analytical expression for the output variance in this case; however, many of the other properties in this section need to be modified (e.g., the variance may not be a strictly increasing function of $\omega_d$).

### 4.2.2 Continuity

The theorem below shows, in two senses, that $V(G)$ is a continuous transformation of $G$. Since there is always uncertainty in $G$ (due to both modeling uncertainty and numerical approximations), continuity of the $V$-transform is a necessary condition for the $V$-transform to be practically useful. In other words, if arbitrarily small changes in $G$ could lead to large changes in $V(G)$, the usefulness of the $V$-transform (and, more fundamentally, the usefulness of variance as a performance measure) would be severely limited.

THEOREM 4.6 *The V-transform is continuous in the following senses:*

(1) $\forall G \in \mathcal{RH}_2$ *and* $\forall \epsilon > 0, \exists \delta > 0$ *such that* $\forall \bar{G} \in \mathcal{RH}_2$,

$$(\|G - \bar{G}\|_2 < \delta) \Rightarrow (\forall \omega_d \in \mathcal{R}_+, |V(G)(\omega_d) - V(\bar{G})(\omega_d)| < \epsilon). \quad (17)$$

(2) $\forall G \in \mathcal{RH}_\infty, \forall \omega_d \in \mathcal{R}_+$, *and* $\forall \epsilon > 0, \exists \delta > 0$ *such that* $\forall \bar{G} \in \mathcal{RH}_\infty$,

$$(\|G - \bar{G}\|_\infty < \delta) \Rightarrow (|V(G)(\omega_d) - V(\bar{G})(\omega_d)| < \epsilon). \quad (18)$$

The first type of continuity in Theorem 4.6 is uniform in $\omega_d$, that is, $\delta$ can be chosen independently of $\omega_d$. The second type of continuity, however, is not uniform in $\omega_d$, and it cannot be strengthened to uniform continuity, as the following example shows:

*Example 4.1* To illustrate the nonuniformity of the second type of continuity in Theorem 4.6, consider the transfer functions

$$G(s) = \frac{1}{s+1}$$

and

$$\bar{G}(s) = \frac{1}{s+1} + \frac{\bar{\delta}}{Ts+1} = (1+\bar{\delta})\frac{((T+\bar{\delta})/(1+\bar{\delta}))s+1}{(s+1)(Ts+1)},$$

where $\bar{\delta}$ and $T$ are positive constants. Note that $G$ and $\bar{G}$ are elements of $\mathcal{RH}_2$, so $\|G-\bar{G}\|_\infty$, $\|G\|_2$, and $\|\bar{G}\|_2$ are all well defined. In fact,

$$\|G-\bar{G}\|_\infty = \left\|\frac{\bar{\delta}}{Ts+1}\right\|_\infty = \bar{\delta}, \tag{19}$$

$$\|G\|_2^2 = \frac{1}{\pi}\int_0^\infty \frac{1}{\omega^2+1}\,d\omega = \frac{1}{2}, \tag{20}$$

and, integrating using partial fractions (for $0<T<1$),

$$\begin{aligned}\|\bar{G}\|_2^2 &= \frac{1}{\pi}\int_0^\infty (1+\bar{\delta})^2 \frac{((T+\bar{\delta})/(1+\bar{\delta}))^2\omega^2+1}{(\omega^2+1)(T^2\omega^2+1)}\,d\omega \\ &= \frac{T^2+T(\bar{\delta}^2+4\bar{\delta}+1)+\bar{\delta}^2}{2T(1+T)}.\end{aligned} \tag{21}$$

Apply Theorem 4.3 and (20)–(21) as follows:

$$\begin{aligned}\lim_{\omega_d\to\infty} |V(G)(\omega_d) - V(\bar{G})(\omega_d)| &= |\|G\|_2^2 - \|\bar{G}\|_2^2| \\ &= \left|\frac{T^2+T(\bar{\delta}^2+4\bar{\delta}+1)+\bar{\delta}^2}{2T(1+T)} - \frac{1}{2}\right|.\end{aligned} \tag{22}$$

The nonuniformity of the continuity follows from (19) and (22), as the following contradiction argument shows: Suppose $\delta$ can be chosen independently of $\omega_d$ in (18). Fix arbitrary $\epsilon > 0$, and fix the corresponding value of $\delta > 0$. Set $\bar{\delta} = \delta/2$. By (19), $\|G - \bar{G}\|_\infty < \delta$ holds for all $T > 0$. Therefore, by (18), it must be that, for all $T > 0$ and for all $\omega_d \in \mathcal{R}_+$, $|V(G)(\omega_d) - V(\bar{G})(\omega_d)| < \epsilon$. But this is impossible since (22) becomes unbounded as $T \to 0$. Hence, there is a contradiction.

To illustrate the nonuniformity graphically, the functions $V(G)$ and $V(\bar{G})$ (for $T = 1$, 0.1, 0.01, and 0.001) are shown in Fig. 10 for $\bar{\delta} = 0.1$. From the figure, it is apparent that $|V(G)(\omega_d) - V(\bar{G})(\omega_d)|$ grows without bound as $T \to 0$ and $\omega_d \to \infty$, even though $\|G - \bar{G}\|_\infty = 0.1$ holds for all $T > 0$.

As a final note on Theorem 4.6, observe that neither type of continuity is uniform in $G$. In fact, by considering a sequence of $G$'s in $\mathcal{RH}_2$ (respectively, $\mathcal{RH}_\infty$) with progressively larger $\mathcal{H}_2$ (respectively, $\mathcal{H}_\infty$) norms, it can be proven that the first type (respectively, the second type) of continuity cannot be strengthened to uniform continuity in $G$.

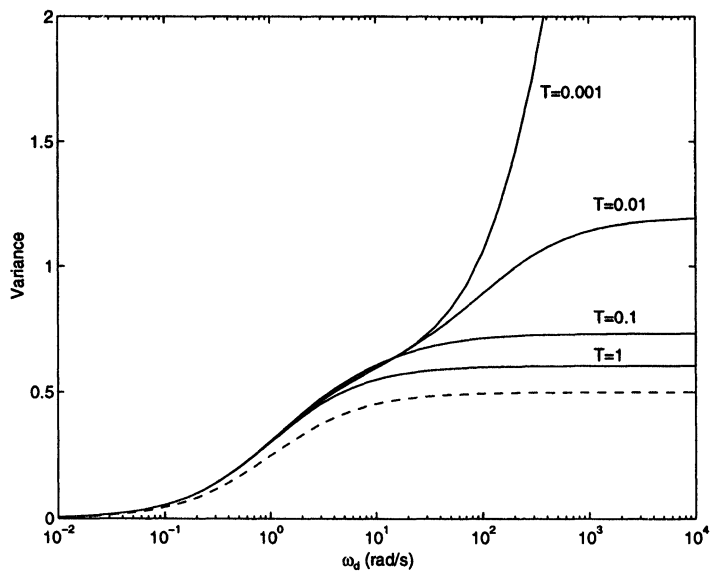


FIGURE 10 $V$-transform of $G$ (dashed) and, for several values of $T$, the $V$-transform of $\bar{G}$ (solid) for Example 4.1.

### 4.2.3 Convexity

$V$-transforms satisfy the following convexity property:

THEOREM 4.7 *The V-transform is a convex operator in the following sense*:

$$\begin{aligned} &\forall G_1, G_2 \in \mathcal{RH}_\infty,\ \forall \lambda \in [0,1],\ \forall \omega_d \in \mathcal{R}_+, \\ &\quad V(\lambda G_1 + (1-\lambda)G_2)(\omega_d) \leq \lambda V(G_1)(\omega_d) + (1-\lambda)V(G_2)(\omega_d). \end{aligned} \tag{23}$$

*Remark 4.5* A useful consequence of this convexity property is that design constraints of the form

$$\forall K > 0,\ \forall \omega_d \in \mathcal{R}_+, \quad V(KG)(\omega_d) \leq B_{\max}(\omega_d, K)$$

(for given positive function $B_{\max}$), or of the form

$$\mathrm{DGM} \geq \mathrm{DGM}_{\min} \quad \text{and} \quad \mathrm{DBM} \geq \mathrm{DBM}_{\min}$$

(for given positive scalars $\mathrm{DGM}_{\min}$ and $\mathrm{DBM}_{\min}$) are *closed-loop convex* (using the terminology of [49]). In other words, the set of Youla parameters corresponding to controllers which satisfy either of these constraints is convex. It follows that the convex programming procedures described in [49] can be used to synthesize controllers which satisfy either (or both) of these constraints.

### 4.2.4 Invertibility

$V(G)$ depends on the magnitude of $G(\mathrm{j}\omega)$ for $\omega \in \mathcal{R}$, but is independent of the phase of $G(\mathrm{j}\omega)$ for $\omega \in \mathcal{R}$. Indeed, the $V$-transform is invariant under all-pass filtering: For any $G \in \mathcal{RH}_\infty$ and any all-pass filter $G_a \in \mathcal{RH}_\infty$, $V(GG_a) = V(G)$. This implies that the $V$-transform is not invertible (with respect to $G$); however, it is conjectured that the $V$-transform is invertible to within an all-pass factor.

## 5 PERFORMANCE LIMITATIONS

The material presented so far has not been dependent on where stable transfer function $G$ originated. For the remainder of the paper, $G$ will be restricted to the form (2). This section addresses the following question: For given $P_1$, $P_2$, $P_3$, $K^*$, and $\omega_d^*$, can the controller $C$ be chosen so that the closed-loop system rejects disturbances with

arbitrarily good robustness (as measured by $DGM_\gamma$ and $DBM_\gamma$)? The answer to this question depends on whether the plant is minimum-phase or nonminimum-phase.[4] Essentially, in the minimum-phase case, the $V$-transform can be pushed down by use of an appropriate high-gain controller; in the nonminimum-phase case, there exists a lower bound on the $V$-transform.

## 5.1 Preliminaries

The methods used to prove the theorems in this section are based on the minimum-variance controller discussion given in [1]. The following results and notation, also adapted from [1], are used throughout. The first lemma gives a useful factorization of transfer functions, the second lemma gives a parameterization of all internally stabilizing controllers in terms of the "Youla parameter" $Q$, and the third lemma gives a decomposition of transfer functions which have no poles on the imaginary axis:

LEMMA 5.1 *Let $H$ be a rational transfer function. Then $H$ can be factored as $H(s) = H_{ap}(s)H_{mp}(s)$, where $H_{ap} \in \mathcal{RH}_\infty$ is an all-pass transfer function and $H_{mp}$ is a transfer function with no zeros in the open right-half plane and with poles coincident with the poles of $H$. The factorization is unique up to sign.*

LEMMA 5.2 *Given $P_1$ and $P_3$ in Fig. 2, define $P = P_1P_3$. Then there exist transfer functions $N, M, X, Y \in \mathcal{RH}_\infty$ such that*

$$P = N/M \quad \text{and} \quad NX + MY = 1 \tag{24}$$

*The closed right-half-plane zeros of $P$ are necessarily the closed right-half-plane zeros of $N$, and the closed right-half-plane poles of $P$ are necessarily the closed right-half-plane zeros of $M$. Moreover, the set of all controllers for which the system is internally stable is*

$$\left\{ \frac{X + MQ}{Y - NQ} : \; Q \in \mathcal{RH}_\infty \right\}. \tag{25}$$

[4] A rational transfer function is said to be *nonminimum-phase* if one or more of its (finite) zeros is in the open right-half plane; otherwise, it is *minimum-phase*. In contrast to definitions used in other papers, the concept of minimum-phasedness used here does not depend on the transfer function poles.

LEMMA 5.3 *Recall that $\mathcal{RH}_2$ denotes the set of strictly proper stable rational transfer functions. Let $\mathcal{RH}_2^\perp$ denote the set of strictly proper rational transfer functions whose poles are all in the open right-half plane. Then the set of all strictly proper rational transfer functions which have no poles on the imaginary axis is $\mathcal{RH}_2 + \mathcal{RH}_2^\perp$, and every $H \in \mathcal{RH}_2 + \mathcal{RH}_2^\perp$ can be decomposed as*

$$H = H_{\text{st}} + H_{\text{un}}, \tag{26}$$

*where $H_{\text{st}} \in \mathcal{RH}_2$ and $H_{\text{un}} \in \mathcal{RH}_2^\perp$. Moreover, for every $H_1 \in \mathcal{RH}_2$ and every $H_2 \in \mathcal{RH}_2^\perp$, $\|H_1 + H_2\|_2^2 = \|H_1\|_2^2 + \|H_2\|_2^2$.*

*Remark 5.1* Algorithms to compute $N$, $M$, $X$, and $Y$ in Lemma 5.2 are given in [1]. The decomposition in (26) can be performed via partial fraction expansion methods.

## 5.2 Minimum-Phase Case

The following theorem summarizes the results in the minimum-phase case. The first two assumptions are introduced for technical reasons; their removal substantially complicates the formulae without adding any significant insight.

THEOREM 5.1 *Assume $P_1$, $P_2$, and $P_3$ in Fig. 2 are given and that they satisfy the following*:

- *none of $P_1$, $P_2$, and $P_3$ have zeros on the imaginary axis,*
- *$P_1$ has no poles on the imaginary axis, and*
- *$P_1$ and $P_3$ have no zeros in the open right-half plane.*

*Let $N$, $M$, $X$, and $Y$ be as in Lemma 5.2. Then the controller corresponding to the Youla parameter*

$$Q(s) = \frac{Y(s)}{N(s)} \frac{1}{(\tau s + 1)^p}, \tag{27}$$

*where $p \geq 0$ is large enough so that $Q$ is proper and $\tau > 0$ is a tunable parameter, satisfies the following properties*:

- *Arbitrarily good nominal disturbance rejection is achievable*:

$$\forall \omega_{\text{d}}^* \in \mathcal{R}_+, \forall \epsilon > 0, \ \exists \bar{\tau} > 0 \ \text{such that} \ \forall \tau \in (0, \bar{\tau}), \ V(G)(\omega_{\text{d}}^*) < \epsilon. \tag{28}$$

- *Let $\Omega$ be an arbitrary bounded set in $\mathcal{R}_+$. Then the V-transform can be "pushed down" arbitrarily close to zero on $\Omega$:*

$$\forall \epsilon > 0,\ \exists \bar{\tau} > 0 \text{ such that } \forall \tau \in (0, \bar{\tau}), \forall \omega_d \in \Omega, \quad V(G)(\omega_d) < \epsilon.$$

- *Let $\mathrm{DGM}_{\min}$ and $\mathrm{DBM}_{\min}$ be arbitrary positive (finite) scalars. Then these robustness margins are achievable, that is,*

$$\forall \omega_d^* > 0,\ \forall \gamma > 0,\ \exists \bar{\tau} > 0 \text{ such that } \forall \tau \in (0, \bar{\tau}),$$
$$\mathrm{DGM}_\gamma \geq \mathrm{DGM}_{\min} \text{ and } \mathrm{DBM}_\gamma \geq \mathrm{DBM}_{\min}.$$

*Remark 5.2* Observe that the controller corresponding to $Q$ in (27) is a high-gain controller: By (25),

$$C(s) = \frac{X(s) + M(s)\big(Y(s)/N(s)\big)\big(1/(\tau s+1)^p\big)}{Y(s) - N(s)\big(Y(s)/N(s)\big)\big(1/(\tau s+1)^p\big)}$$
$$= \frac{1}{\tau s} \frac{(\tau s+1)^p N(s)X(s) + M(s)Y(s)}{\left[\sum_{i=1}^{p} p!/\big(i!(i-1)!\big)(\tau s)^{i-1}\right] N(s)Y(s)}.$$

In the case where $P_3P_1$ is both minimum-phase and stable, it is possible to use $N = P_3P_1$, $M = 1$, $X = 0$, and $Y = 1$. Then the controller simplifies further to

$$\frac{1}{[(\tau s+1)^p - 1]P_3P_1},$$

so the closed-loop poles are the (canceled) poles and zeros of $P_3P_1$ together with $p$ poles at $s = -1/\tau$.

*Remark 5.3* The high-gain controller in Theorem 5.1 theoretically exhibits excellent disturbance rejection properties, but in practice there would be problems associated with the resulting high bandwidth system (e.g., signals may saturate, there may be stability problems due to neglected high-frequency dynamics and time delays, sensor noise may be amplified). Moreover, the resulting pole-zero cancelations (see the previous remark) are often undesirable in practice.

*Remark 5.4* A minimum-variance controller can also be considered to be a maximum-$\mathrm{DGM}_\gamma$ controller.

### 5.3 NonMinimum-Phase Case

The following result is the nonminimum-phase version of Theorem 5.1:

THEOREM 5.2 *Assume $P_1$, $P_2$, and $P_3$ in Fig. 2 are given and that they satisfy the following*:

- *none of $P_1$, $P_2$, and $P_3$ have zeros on the imaginary axis,*
- *$P_1$ has no poles on the imaginary axis, and*
- *$P_1$ or $P_3$ has zeros in the open right-half plane.*

*Then there are limitations on nominal disturbance rejection and on the achievable robustness margins*:

- *Fix $\omega_d^* > 0$, define $N$, $M$, $X$, and $Y$ as in Lemma 5.2, and define $\bar{F} = \omega_d^*/(s+\omega_d^*)$, $V = P_3P_2\bar{F}MY$, $U = P_3P_2\bar{F}MN$, and $\alpha = \|(U_{ap}^{-1}V)_{un}\|_2^2$. Then $\alpha > 0$ and, for all internally stabilizing controllers,*

$$V(G)(\omega_d^*) \geq \alpha. \tag{29}$$

*Moreover, the controller corresponding to the Youla parameter*

$$Q(s) = U_{mp}^{-1}(U_{ap}^{-1}V)_{st}\frac{1}{(\tau s+1)^p}, \tag{30}$$

*where $p \geq 0$ is large enough so that $Q$ is proper and $\tau > 0$ is a tunable parameter, satisfies the following property*:

$$\forall \epsilon > 0,\ \exists \bar{\tau} > 0 \text{ such that } \forall \tau \in (0, \bar{\tau}),\quad |V(G)(\omega_d^*) - \alpha| < \epsilon. \tag{31}$$

- *There exists a function $B_{\min}: \mathcal{R}_+ \to \mathcal{R}_+ : \omega_d \mapsto B_{\min}(\omega_d)$ that satisfies the following*:
  - *$B_{\min}$ is a strictly increasing analytic function with $B_{\min}(0) = 0$.*
  - *For all internally stabilizing controllers and for all $\omega_d \in \mathcal{R}_+$, $V(G)(\omega_d) \geq B_{\min}(\omega_d)$.*
  - *For all $\omega_d^* > 0$, the $V$-transform of the system with Youla parameter (30) is tangent to $B_{\min}$ at $\omega_d = \omega_d^*$ in the limit $\tau \to 0$.*
- *For all $\omega_d^* > 0$ and all $\gamma > 0$, there exists a finite scalar $\mathrm{DGM}_{\max}$ such that, for all internally stabilizing controllers, $\mathrm{DGM}_\gamma \leq \mathrm{DGM}_{\max}$.*
- *For all $\omega_d^* > 0$, there exists a $\bar{\gamma} > 0$ and a finite scalar $\mathrm{DBM}_{\max}$ such that, for all internally stabilizing controllers and for all $\gamma \in (0, \bar{\gamma})$, $\mathrm{DBM}_\gamma \leq \mathrm{DBM}_{\max}$.*

*Remark 5.5* The notion that arbitrarily good performance can be attained for minimum-phase systems but not for nonminimum-phase systems appears in other lines of research. Examples include work on the *perfect robust servomechanism* problem [88,89] and the aiming control problem [13,17]. Other examples are cited in [89].

Function $B_{\min}$ in the above theorem plays the role of a *performance limitation curve*. It can be characterized explicitly in several cases. For example, in the case where $P_1P_3$ has a single nonminimum-phase zero, the following result holds; it can be assumed without loss of generality that $P_2$ has no zeros in the open right-half-plane, and, as usual, the imaginary axis assumptions can be weakened.

THEOREM 5.3 *Assume that $P_1$, $P_2$, and $P_3$ in Fig. 2 are given and they satisfy the following*:

- *$P_1$ and $P_3$ have no zeros on the imaginary axis,*
- *$P_2$ has no zeros in the closed right-half-plane,*
- *$P_1$ has no poles on the imaginary axis, and*
- *$P \triangleq P_1P_3$ has exactly one nonminimum-phase zero at $s=z$ for $z>0$.*

*Also suppose that $P_1$ has $n_1 \geq 0$ unstable poles at $s=p_{1,i}$ for $i=1,\ldots,n_1$ and $P_3$ has $n_3 \geq 0$ unstable poles at $s=p_{3,i}$ for $i=1,\ldots,n_3$. Let $N$, $M$, $X$, and $Y$ be as in Lemma 5.2. Then the performance limitation curve has the form*

$$B_{\min}(\omega_d) = \beta(z)F^2(s)|_{s=z},$$

*where $\beta(z)$ is a constant that is independent of $\omega_d$ and is computed as follows*:

- *If the nonminimum-phase zero is in $P_3$, define the following stable minimum-phase transfer functions*:

$$\bar{P}_3(s) = \frac{[\Pi_{i=1}^{n_3}(s-p_{3,i})]}{s-z}P_3(s) \text{ and } \bar{M}(s) = \frac{M(s)}{[\Pi_{i=1}^{n_3}(s-p_{3,i})][\Pi_{i=1}^{n_1}(s-p_{1,i})]}.$$

*Then*

$$\beta(z) = 8z^3\left[\prod_{i=1}^{n_1}(z+p_{1,i})^2\right]\bar{P}_3^2(z)P_2^2(z)\bar{M}^2(z)Y^2(z).$$

- *If the nonminimum-phase zero is in $P_1$, define the following stable minimum-phase transfer functions*:

$$\bar{P}_3(s) = \left[\prod_{i=1}^{n_3}(s - p_{3,i})\right] P_3(s) \quad \text{and} \quad \bar{M}(s) = \frac{M(s)}{[\Pi_{i=1}^{n_3}(s - p_{3,i})][\Pi_{i=1}^{n_1}(s - p_{1,i})]}.$$

*Then*

$$\beta(z) = 2z\left[\prod_{i=1}^{n_1}(z + p_{1,i})^2\right] \bar{P}_3^2(z) P_2^2(z) \bar{M}^2(z) Y^2(z).$$

*Remark 5.6* Analogous results to Theorem 5.3 can be derived for the multiple nonminimum-phase zero case, but the results get progressively more complicated as the number of nonminimum-phase zeros increases. Also, a study was performed on the effect of moving the nonminimum-phase zero $z$ closer to the origin. The details are omitted, but essentially three distinct behaviors exist: The $B_{\min}$ curve tends to zero uniformly in $z$; the $B_{\min}$ curve tends to zero pointwise, but not uniformly, in $z$; or the $B_{\min}$ curve becomes unbounded as $z \to 0$. Which behavior occurs depends on the number of integrators in $P_3$ and differentiators in $P_2$, the way in which $z$ enters the plant (e.g., as $(s - z)/(s + z)$ or just $(s - z)$), and whether $z$ is a part of $P_1$ or $P_3$.

## 6 EXAMPLES

The following two academic examples illustrate application of the tools and theory developed in this paper.

*Example 6.1* Reconsider Example 1.1 in which the plant is

$$P_1(s) = 1, \quad P_2(s) = 1, \quad P_3(s) = \frac{10}{s + 1},$$

and the two controllers under consideration are

$$C_1(s) = \frac{0.5(s + 2)}{s} \quad \text{and} \quad C_2(s) = 0.86.$$

Recall that the nominal disturbance parameters are $\omega_d^* = 1$ rad/s and $K^* = 1$, and that the performance threshold is $\gamma = 2.5$.

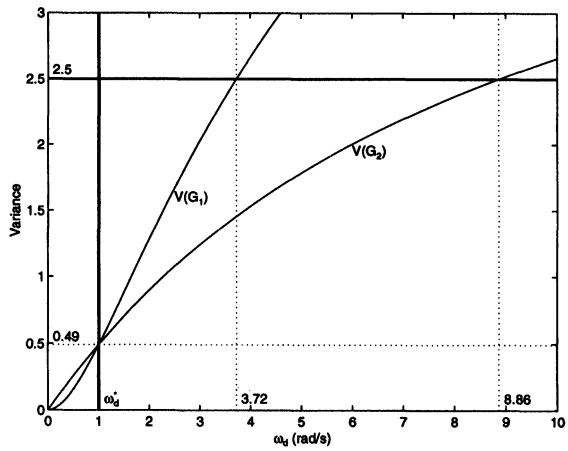


FIGURE 11 $V$-transforms of $G_1$ and $G_2$ for the simple autopilot example.

To evaluate the performance of the controllers with respect to disturbance rejection in the face of uncertainty in $\omega_d$, consider the plots of $V(G_1)$ and $V(G_2)$ in Fig. 11. Since the controller gains were selected so that the nominal output variance corresponding to $C_2$ is the same as that corresponding to $C_1$, the $V$-transforms are equal at $\omega_d = \omega_d^*$. For $\omega_d < \omega_d^*$, controller $C_1$, the integral controller, is the better controller; for $\omega_d > \omega_d^*$, controller $C_2$, the nonintegral controller, is better. We can quantify the superiority of the nonintegral controller (with respect to performance in the face of increasing $\omega_d$) by computing the robustness measures: From the figure, the margins for $C_1$ are

$$\text{DBM}_\gamma = \frac{3.72}{1} = 3.72 \quad \text{and} \quad \text{DGM}_\gamma = \sqrt{\frac{2.5}{0.49}} = 2.26$$

and the margins for $C_2$ are

$$\text{DBM}_\gamma = \frac{8.86}{1} = 8.86 \quad \text{and} \quad \text{DGM}_\gamma = \sqrt{\frac{2.5}{0.49}} = 2.26.$$

Hence, the nonintegral controller has a significantly larger disturbance bandwidth margin than the integral controller.

*Example 6.2* Consider the following nonminimum-phase plant:

$$P_1(s) = 1, \quad P_2(s) = 1, \quad P_3(s) = \frac{s-a}{a(s+1)^2},$$

where $a > 0$ is the location of the nonminimum-phase zero. We consider below the development of the minimum variance controller and performance limitation curve.

The most obvious choice for $N$, $M$, $X$, and $Y$ is

$$N(s) = \frac{s-a}{a(s+1)^2}, \quad M(s) = 1, \quad X(s) = 0, \quad Y(s) = 1.$$

To compute the minimum-variance controller, (30) needs to be evaluated. First compute

$$V = P_3 P_2 \bar{F} M Y = \frac{s-a}{a(s+1)^2} \frac{\omega_d^*}{s+\omega_d^*}$$

and

$$U = P_3 P_2 \bar{F} M N = \frac{(s-a)^2}{a^2(s+1)^4} \frac{\omega_d^*}{s+\omega_d^*}.$$

Factor $U$ as $U = U_{ap} U_{mp}$, where

$$U_{ap} = \frac{(s-a)^2}{(s+a)^2} \quad \text{and} \quad U_{mp} = \frac{(s+a)^2 \omega_d^*}{a^2(s+1)^4(s+\omega_d^*)},$$

and decompose $U_{ap}^{-1} V$ into $(U_{ap}^{-1} V)_{un} + (U_{ap}^{-1} V)_{st}$ as follows:

$$U_{ap}^{-1} V = \frac{(s+a)^2 \omega_d^*}{a(s-a)(s+1)^2(s+\omega_d^*)} = \frac{\Gamma_1}{s-a} + \frac{\Gamma_2}{(s+1)^2(s+\omega_d^*)},$$

where

$$\Gamma_1 = \frac{4a\omega_d^*}{(a+1)^2(a+\omega_d^*)} \quad \text{and} \quad \Gamma_2 = \frac{\omega_d^*}{a(a+1)^2(a+\omega_d^*)}(\beta_1 s^2 + \beta_2 s + \beta_3), \tag{32}$$

where the constants $\beta_1$, $\beta_2$, and $\beta_3$ are

$$\beta_1 = -4a^2,$$

$$\beta_2 = -3a^3 - 3a^2(\omega_d^* + 2) + a(2\omega_d^* + 1) + \omega_d^*,$$

$$\beta_3 = -a^4 - a^3(\omega_d^* + 2) - a^2(2\omega_d^* + 1) + a(3\omega_d^*).$$

Then the Youla parameter corresponding to the (suboptimal) minimum-variance controller is

$$Q(s) = U_{\text{mp}}^{-1}(U_{\text{ap}}^{-1}V)_{\text{st}}\frac{1}{(\tau s+1)^p} = \frac{a(s+1)^2(\beta_1 s^2+\beta_2 s+\beta_3)}{(s+a)^2(a+1)^2(a+\omega_{\text{d}}^*)(\tau s+1)^p}.$$

To make $Q$ and the corresponding controller proper, select $p=2$. By Theorem 5.2, the minimum variance, as a function of $a$ and $\omega_{\text{d}}^*$, is

$$\|(U_{\text{ap}}^{-1}V)_{\text{un}}\|_2^2 = \left\|\frac{\Gamma_1}{s-a}\right\|_2^2 = \frac{\Gamma_1^2}{2a} = \frac{8a(\omega_{\text{d}}^*)^2}{(a+1)^4(a+\omega_{\text{d}}^*)^2}. \tag{33}$$

(Alternatively, Theorem 5.3 can be used to derive this expression.)

For $a=1$ and $\omega_{\text{d}}^* = 1$ rad/s, Figs. 12 and 13 show the Bode magnitude plot of the closed-loop transfer function $G$ and the $V$-transform of $G$, respectively, for several values of $\tau$. The performance limitation curve in (33) (for $a=1$ and using $\omega_{\text{d}}$ in place of $\omega_{\text{d}}^*$) is included in the $V$-transform plot. As expected, in the limit $\tau \to 0$, the $V$-transform is

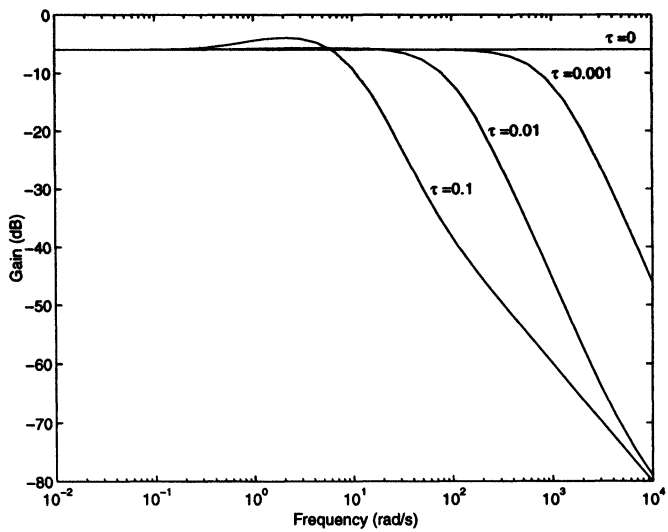


FIGURE 12 Bode magnitude plot of $G$ for several values of $\tau$ in Example 6.2. Both $a$ and $\omega_{\text{d}}^*$ are set to one.

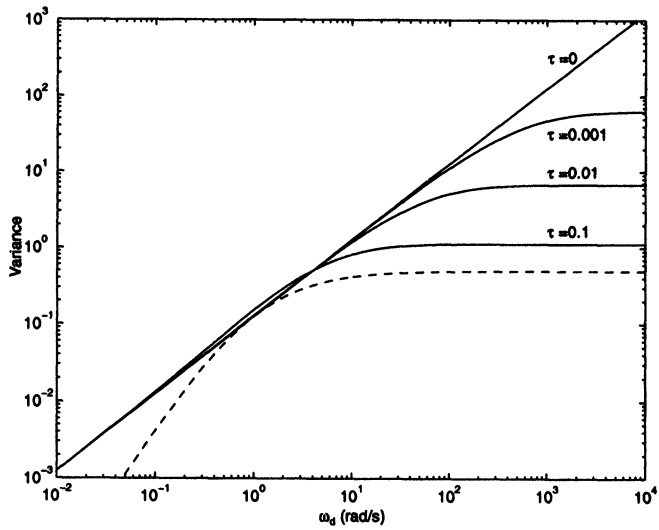


FIGURE 13 $V$-transform of $G$ for several values of $\tau$ in Example 6.2. The dashed line is the performance limitation curve in (33). Both $a$ and $\omega_d^*$ are set to one.

tangent to the performance limitation curve at $\omega_d = \omega_d^*$. Also observe that, as $\tau \to 0$, the system bandwidth becomes infinite and $|G(j\omega)|$ tends (pointwise) to a curve that is nonzero everywhere. In fact, a calculation indicates that, as $\tau \to 0$, $G$ approaches the transfer function

$$\frac{(s-a)[(s+a)^2(a+1)^2(a+\omega_d^*) - (s-a)(\beta_1 s^2 + \beta_2 s + \beta_3)]}{a(s+1)^2(s+a)^2(a+1)^2(a+\omega_d^*)},$$

which is biproper (and, moreover, if $a = \omega_d^*$, all-pass). Consequently, $V(G)$ tends to an unbounded function as $\tau \to 0$ (recall the last point of Theorem 4.3).

## 7 CONCLUSIONS AND FUTURE WORK

This paper introduced the $V$-transform as a new mathematical tool for the robustness analysis of feedback control systems with respect to uncertainty in the disturbance gain and bandwidth. Mathematical properties of $V$-transforms were investigated, and the notions of

disturbance gain margin and disturbance bandwidth margin were defined. It was argued by example that the use of $V$-transforms and these new margins gives insight into system behavior that is not apparent when restricted to the classical analysis tools (Bode plots, gain and phase margins, etc.). Finally, it was shown that there exists a robustness performance limitation in the case where the plant is nonminimum-phase, but no such limitation if the plant is minimum-phase.

The results from this paper have been applied to an aircraft autopilot system to analyze system performance in the face of uncertainty in turbulence scale [90]. Other potential applications being considered include the control of ships (where waves, wind, and current act as disturbances), automobiles (where wind, road roughness, and engine vibrations act as disturbances), actively controlled buildings (where earthquakes act as disturbances), and manufacturing systems (where machine-wear and variations in environmental conditions act as disturbances). Theoretical work being developed includes determination of performance limitations under practical system constraints (e.g., constraints on the closed-loop system bandwidth and stability margins).

## APPENDIX

### Proof of Theorem 4.1

Realization (14) is derived first. On noting that

$$F(s) = \omega_d/(s+\omega_d) = \left[\begin{array}{c|c} -\omega_d & \omega_d \\ \hline 1 & 0 \end{array}\right](s),$$

it follows that

$$G(s)\cdot F(s) = \left[\begin{array}{c|c} A & B \\ \hline C & D \end{array}\right](s)\cdot\left[\begin{array}{c|c} -\omega_d & \omega_d \\ \hline 1 & 0 \end{array}\right](s)$$

$$= \left[\begin{array}{cc|c} A & B & 0 \\ 0 & -\omega_d & \omega_d \\ \hline C & D & 0 \end{array}\right](s). \tag{34}$$

Let $L$ denote the observability Grammian of this realization of GF. Partition $L$ as

$$L = \begin{bmatrix} L_1 & L_2^{\mathrm{T}} \\ L_2 & L_3 \end{bmatrix},$$

where $L_3$ is a scalar. Then, by the definition of $V(G)(\omega_{\mathrm{d}})$ and by Lemma 4.1 applied to $GF \in \mathcal{RH}_2$,

$$V(G)(\omega_{\mathrm{d}}) = \|GF\|_2^2 - [0 \quad \omega_{\mathrm{d}}] L \begin{bmatrix} 0 \\ \omega_{\mathrm{d}} \end{bmatrix} = \omega_{\mathrm{d}}^2 L_3. \tag{35}$$

We now solve for $L_3$ for substitution in (35). The Lyapunov equation for the observability Grammian of

$$\left( [C \quad D], \begin{bmatrix} A & B \\ 0 & -\omega_{\mathrm{d}} \end{bmatrix} \right)$$

is

$$\begin{bmatrix} A & B \\ 0 & -\omega_{\mathrm{d}} \end{bmatrix}^{\mathrm{T}} \begin{bmatrix} L_1 & L_2^{\mathrm{T}} \\ L_2 & L_3 \end{bmatrix} + \begin{bmatrix} L_1 & L_2^{\mathrm{T}} \\ L_2 & L_3 \end{bmatrix} \begin{bmatrix} A & B \\ 0 & -\omega_{\mathrm{d}} \end{bmatrix} + [C \quad D]^{\mathrm{T}} [C \quad D] = 0.$$

This matrix equation is equivalent to the following three equations:

$$A^{\mathrm{T}} L_1 + L_1 A + C^{\mathrm{T}} C = 0, \tag{36}$$

$$B^{\mathrm{T}} L_1 - \omega_{\mathrm{d}} L_2 + L_2 A + DC = 0, \tag{37}$$

$$B^{\mathrm{T}} L_2^{\mathrm{T}} - \omega_{\mathrm{d}} L_3 + L_2 B - \omega_{\mathrm{d}} L_3 + D^2 = 0. \tag{38}$$

Equation (36) indicates that $L_1$ is the observability Grammian of $(C, A)$; denote this Grammian by $L_{\mathrm{o}}$ By the stability of $G$, $\omega_{\mathrm{d}}$ is not an eigenvalue of $A$; hence, $(A - \omega_{\mathrm{d}} I)^{-1}$ exists, and solving for $L_2$ in (37) yields

$$L_2 = (-B^{\mathrm{T}} L_{\mathrm{o}} - DC)(A - \omega_{\mathrm{d}} I)^{-1}. \tag{39}$$

Next, solve for scalar $L_3$ in (38) and substitute for $L_2$ using (39) to obtain

$$L_3 = \frac{1}{2\omega_d} D^2 - \frac{1}{\omega_d}(B^T L_o + DC)(A - \omega_d I)^{-1} B.$$

Use this to substitute for $L_3$ in (35):

$$V(G)(\omega_d) = \tfrac{1}{2}\omega_d D^2 - \omega_d (B^T L_o + DC)(A - \omega_d I)^{-1} B.$$

Use the fact that $A$ is invertible to rewrite this as

$$V(G)(\omega_d) = \frac{1}{2}\omega_d D^2 - (B^T L_o + DC)\left(\frac{1}{\omega_d} I - A^{-1}\right)^{-1} A^{-1} B. \tag{40}$$

Now recognize (40) as the parallel connection of

$$\frac{1}{2}\omega_d D^2 = \left[\begin{array}{c|c} 0 & D^2/2 \\ \hline 1 & 0 \end{array}\right]\left(\frac{1}{\omega_d}\right)$$

and

$$-(B^T L_o + DC)\left(\frac{1}{\omega_d} I - A^{-1}\right)^{-1} A^{-1} B$$

$$= \left[\begin{array}{c|c} A^{-1} & A^{-1}B \\ \hline -(B^T L_o + DC) & 0 \end{array}\right]\left(\frac{1}{\omega_d}\right).$$

Thus,

$$V(G)(\omega_d) = \left[\begin{array}{c|c} 0 & D^2/2 \\ \hline 1 & 0 \end{array}\right]\left(\frac{1}{\omega_d}\right) + \left[\begin{array}{c|c} A^{-1} & A^{-1}B \\ \hline -(B^T L_o + DC) & 0 \end{array}\right]\left(\frac{1}{\omega_d}\right)$$

$$= \left[\begin{array}{cc|c} A^{-1} & 0 & A^{-1}B \\ 0 & 0 & D^2/2 \\ \hline -(B^T L_o + DC) & 1 & 0 \end{array}\right]\left(\frac{1}{\omega_d}\right), \tag{41}$$

which is formula (14). To obtain (15), manipulate (40) as follows:

$$
\begin{aligned}
V(G)(\omega_d) &= \frac{1}{2}\omega_d D^2 + (B^T L_o + DC)\left(I - \frac{1}{\omega_d}A\right)^{-1} B \\
&= \frac{1}{2}\omega_d D^2 + (B^T L_o + DC)B \\
&\quad + (B^T L_o + DC)\frac{1}{\omega_d}A\left(I - \frac{1}{\omega_d}A\right)^{-1} B \\
&= \frac{1}{2}\omega_d D^2 + (B^T L_o + DC)B + (B^T L_o + DC)A(\omega_d I - A)^{-1} B \\
&= \frac{1}{2}\omega_d D^2 + \left[\begin{array}{c|c} A & B \\ \hline (B^T L_o + DC)A & (B^T L_o + DC)B \end{array}\right](\omega_d),
\end{aligned}
$$

where the second equality follows from the identity $(I-M)^{-1} = I + M(I-M)^{-1}$.

**Proof of Corollary 4.1**

When $D=0$, (14) simplifies as follows:

$$
\left[\begin{array}{c|c} \hat{A} & \hat{B} \\ \hline \hat{C} & 0 \end{array}\right]\left(\frac{1}{\omega_d}\right) = \left[\begin{array}{cc|c} A^{-1} & 0 & A^{-1}B \\ 0 & 0 & 0 \\ \hline -B^T L_o & 1 & 0 \end{array}\right]\left(\frac{1}{\omega_d}\right)
$$

$$
= \begin{bmatrix} -B^T L_o & 1 \end{bmatrix}\begin{bmatrix} (1/\omega_d)I - A^{-1} & 0 \\ 0 & (1/\omega_d) \end{bmatrix}^{-1}\begin{bmatrix} A^{-1}B \\ 0 \end{bmatrix}
$$

$$
= -B^T L_o\left(\frac{1}{\omega_d}I - A^{-1}\right)^{-1} A^{-1}B = \left[\begin{array}{c|c} A^{-1} & A^{-1}B \\ \hline -B^T L_o & 0 \end{array}\right]\left(\frac{1}{\omega_d}\right).
$$

When $D=0$, realization (15) immediately simplifies.

**Proof of Theorem 4.2**

To prove the analyticity of $V(G)$, note from Theorem 4.1 that $V(G)$ is the ratio of polynomials in $\omega_d$, where the denominator term is nonzero

for all $\omega_d \in \mathcal{R}_+$; all such rational functions are analytic. To derive the given derivatives, first use Theorem 4.1 to obtain

$$V(G)(\omega_d) = \left[\begin{array}{c|c} \bar{A} & \bar{B} \\ \hline \bar{C} & \bar{D} \end{array}\right](\omega_d) + \frac{1}{2}\omega_d D^2 = \bar{D} + \bar{C}(\omega_d I - \bar{A})^{-1}\bar{B} + \frac{1}{2}\omega_d D^2.$$

The desired derivatives follow by simple matrix calculus (see [91], for example).

**Proof of Theorem 4.3**

The property $V(G)(0) = 0$ follows from the definition of $V(G)$:

$$\begin{aligned} V(G)(0) &= \lim_{\omega_d \to 0} \frac{1}{\pi} \int_0^\infty |G(j\omega)|^2 \frac{\omega_d^2}{\omega^2 + \omega_d^2}\, d\omega \\ &= \lim_{\omega_d \to 0} \frac{\omega_d}{\pi} \int_0^\infty |G(j\omega_d\bar{\omega})|^2 \frac{1}{\bar{\omega}^2 + 1}\, d\bar{\omega}. \end{aligned}$$

This limit is bounded below by zero since the integrand is nonnegative. It is also bounded above by zero since $G \in \mathcal{RH}_\infty$ implies that $\|G\|_\infty < \infty$, from which it follows that

$$\lim_{\omega_d \to 0} \frac{\omega_d}{\pi} \int_0^\infty |G(j\omega_d\bar{\omega})|^2 \frac{1}{\bar{\omega}^2 + 1}\, d\bar{\omega} \le \lim_{\omega_d \to 0} \frac{\omega_d}{\pi} \|G\|_\infty^2 \int_0^\infty \frac{1}{\bar{\omega}^2 + 1} d\bar{\omega} = 0.$$

Hence, $V(G)(0) = 0$. (An alternative proof is to substitute $\omega_d = 0$ in (15).)

To show the next two points in the theorem, use the differentiability of $V(G)(\omega_d)$ proven in Theorem 4.2 as follows: For all $\omega_d \in \mathcal{R}_+$,

$$\begin{aligned} \frac{d}{d\omega_d} V(G)(\omega_d) &= \frac{1}{\pi} \frac{d}{d\omega_d} \int_0^\infty |G(j\omega)|^2 \frac{\omega_d^2}{\omega^2 + \omega_d^2}\, d\omega \\ &= \frac{1}{\pi} \int_0^\infty |G(j\omega)|^2 \frac{d}{d\omega_d} \left( \frac{\omega_d^2}{\omega^2 + \omega_d^2} \right) d\omega \\ &= \frac{1}{\pi} \int_0^\infty |G(j\omega)|^2 \frac{2\omega^2 \omega_d}{(\omega^2 + \omega_d^2)^2}\, d\omega \\ &= \frac{2}{\pi} \int_0^\infty |G(j\omega_d\bar{\omega})|^2 \frac{\bar{\omega}^2}{(\bar{\omega}^2 + 1)^2}\, d\bar{\omega}. \end{aligned} \tag{42}$$

To justify the interchange of differentiation and integration operations above, invoke Theorem 17.3e in [92]. (Essentially, the interchange is

valid because $\|G\|_\infty < \infty$ and because

$$\int_0^\infty \frac{\bar{\omega}^2}{(\bar{\omega}^2+1)^2}\,\mathrm{d}\omega \tag{43}$$

converges uniformly with respect to $\omega_\mathrm{d}$ in every closed interval in $\mathcal{R}_+$; In fact, (43) is independent of $\omega_\mathrm{d}$ and equals $\pi/4$. The notion of uniform convergence of integrals is defined in [92].) Taking the limit as $\omega_\mathrm{d} \to 0$ in (42) yields

$$\begin{aligned}\frac{\mathrm{d}}{\mathrm{d}\omega_\mathrm{d}} V(G)(0) &= \lim_{\omega_\mathrm{d}\to 0} \frac{2}{\pi}\int_0^\infty |G(\mathrm{j}\omega_\mathrm{d}\bar{\omega})|^2 \frac{\bar{\omega}^2}{(\bar{\omega}^2+1)^2}\,\mathrm{d}\bar{\omega} \\ &= \frac{2|G(0)|^2}{\pi}\int_0^\infty \frac{\bar{\omega}^2}{(\bar{\omega}^2+1)^2}\,\mathrm{d}\bar{\omega} = \frac{|G(0)|^2}{2},\end{aligned}$$

which proves the second point in the theorem. (The justification for taking the limit under the integral sign is found in Theorem 17.3c in [92].) The third point in the theorem also follows from (42) since, for nonzero $G$ and all $\omega_\mathrm{d} \in \mathcal{R}_+$, the integrand is positive almost everywhere. Finally, to derive the limiting behavior of $V(G)(\omega_\mathrm{d})$ as $\omega_\mathrm{d} \to \infty$, use realization (15) from Theorem 4.1 to obtain $V(G)(\omega_\mathrm{d}) \to \bar{D} + \omega_\mathrm{d} D^2/2 = B^\mathrm{T} L_\mathrm{o} B + \mathrm{DCB} + \omega_\mathrm{d} D^2/2$.

**Proof of Theorem 4.4**

The result follows immediately from the following facts:

- $V(G)(\omega_\mathrm{d})$ is a strictly increasing continuous function of $\omega_\mathrm{d}$ (see Theorems 4.2 and 4.3),
- $V(G)(0) = 0$ (see Theorem 4.3),
- If $G \in \mathcal{RH}_2$ then $\sup_{\omega_\mathrm{d}\in\mathcal{R}_+} V(G)(\omega_\mathrm{d}) = \|G\|_2^2$; otherwise, $G$ is unbounded (see Theorem 4.3 and Lemma 4.1).

**Proof of Theorem 4.5**

From the definition of $V(G)$, for all $\omega_\mathrm{d} \in \mathcal{R}_+$,

$$\begin{aligned}V(\alpha G)(\omega_\mathrm{d}) &= \frac{1}{\pi}\int_0^\infty |\alpha G(\mathrm{j}\omega)|^2 \frac{\omega_\mathrm{d}^2}{\omega^2+\omega_\mathrm{d}^2}\,\mathrm{d}\omega \\ &= |\alpha|^2 \frac{1}{\pi}\int_0^\infty |G(\mathrm{j}\omega)|^2 \frac{\omega_\mathrm{d}^2}{\omega^2+\omega_\mathrm{d}^2}\,\mathrm{d}\omega = \alpha^2 V(G)(\omega_\mathrm{d}).\end{aligned}$$

**Proof of Theorem 4.6**

Introduce the following notation for the proof: For each $\omega_d \in \mathcal{R}_+$, define $\|\cdot\|_{\omega_d}: \mathcal{RH}_\infty \to \mathcal{R}$ by $\|M\|_{\omega_d} = \|MF\|_2$. Note that $\forall M \in \mathcal{RH}_\infty$ and $\forall \omega_d \in \mathcal{R}_+$, $V(M)(\omega_d) = \|MF\|_2^2 = \|M\|_{\omega_d}^2$. It is simple to verify that, for each $\omega_d \in \mathcal{R}_+$, $\|\cdot\|_{\omega_d}$ is a norm.

Recall that every norm is uniformly continuous: For any space $V$ with norm $\|\cdot\|$, the triangle inequality yields $\forall x, \bar{x} \in V$, $|\|x\| - \|\bar{x}\|| \leq \|x - \bar{x}\|$, which implies that

$$\forall \epsilon^* > 0,\ \forall x, \bar{x} \in V,\quad (\|x - \bar{x}\| < \epsilon^*) \ \Rightarrow\ (|\|x\| - \|\bar{x}\|| < \epsilon^*). \tag{44}$$

Applying (44) to the norm just defined yields

$$\begin{aligned} &\forall \omega_d \in \mathcal{R}_+,\ \forall \epsilon^* > 0,\ \forall G, \bar{G} \in \mathcal{RH}_\infty, \\ &\quad (\|G - \bar{G}\|_{\omega_d} < \epsilon^*) \ \Rightarrow\ (\,|\|G\|_{\omega_d} - \|\bar{G}\|_{\omega_d}| < \epsilon^*). \end{aligned} \tag{45}$$

The first continuity statement will now be proved. Since $\mathcal{RH}_2 \subset \mathcal{RH}_\infty$, (45) implies

$$\begin{aligned} &\forall \omega_d \in \mathcal{R}_+,\ \forall \epsilon^* > 0,\ \forall G, \bar{G} \in \mathcal{RH}_2, \\ &\quad (\|G - \bar{G}\|_{\omega_d} < \epsilon^*) \ \Rightarrow\ (|\|G\|_{\omega_d} - \|\bar{G}\|_{\omega_d}| < \epsilon^*), \end{aligned}$$

or, equivalently,

$$\begin{aligned} &\forall \epsilon^* > 0,\ \forall G, \bar{G} \in \mathcal{RH}_2,\ \forall \omega_d \in \mathcal{R}_+, \\ &\quad (\|G - \bar{G}\|_{\omega_d} < \epsilon^*) \ \Rightarrow\ (|\|G\|_{\omega_d} - \|\bar{G}\|_{\omega_d}| < \epsilon^*). \end{aligned} \tag{46}$$

Next, observe that, for all $M \in \mathcal{RH}_2$ and all $\omega_d \in \mathcal{R}_+$,

$$\begin{aligned} \|M\|_{\omega_d}^2 = \|MF\|_2^2 &= \frac{1}{\pi}\int_0^\infty |M(j\omega)|^2 \frac{\omega_d^2}{\omega^2 + \omega_d^2}\,d\omega \\ &\leq \frac{1}{\pi}\int_0^\infty |M(j\omega)|^2 d\omega = \|M\|_2^2, \end{aligned}$$

that is,

$$\forall M \in \mathcal{RH}_2,\ \forall \omega_d \in \mathcal{R}_+,\quad \|M\|_{\omega_d} \leq \|M\|_2. \tag{47}$$

Combining (46) and (47) results in

$$\forall \epsilon^* > 0,\ \forall G, \bar{G} \in \mathcal{RH}_2,\ \forall \omega_d \in \mathcal{R}_+,$$
$$(\|G - \bar{G}\|_2 < \epsilon^*) \Rightarrow (|\|G\|_{\omega_d} - \|\bar{G}\|_{\omega_d}| < \epsilon^*),$$

or, equivalently,

$$\forall \epsilon^* > 0,\ \forall G, \bar{G} \in \mathcal{RH}_2$$
$$(\|G - \bar{G}\|_2 < \epsilon^*) \Rightarrow (\forall \omega_d \in \mathcal{R}_+,\ |\|G\|_{\omega_d} - \|\bar{G}\|_{\omega_d}| < \epsilon^*). \quad (48)$$

Now fix $G \in \mathcal{RH}_2$, fix $\epsilon > 0$, and define both $\alpha = 2\|G\|_2 + 2$ and $\delta = \min(1, \epsilon/\alpha)$. Use $\epsilon^* = \epsilon/\alpha$ in (48) to obtain

$$\forall \bar{G} \in \mathcal{RH}_2,\ \left(\|G - \bar{G}\|_2 < \frac{\epsilon}{\alpha}\right) \Rightarrow \left(\forall \omega_d \in \mathcal{R}_+,\ |\|G\|_{\omega_d} - \|\bar{G}\|_{\omega_d}| < \frac{\epsilon}{\alpha}\right),$$

from which it follows that

$$\forall \bar{G} \in \mathcal{RH}_2,\quad (\|G - \bar{G}\|_2 < \delta) \Rightarrow \left(\forall \omega_d \in \mathcal{R}_+,\ |\|G\|_{\omega_d} - \|\bar{G}\|_{\omega_d}| < \frac{\epsilon}{\alpha}\right). \quad (49)$$

The first continuity result follows: If $\bar{G} \in \mathcal{RH}_2$ satisfies $\|G - \bar{G}\|_2 < \delta$, then, for all $\omega_d \in \mathcal{R}_+$,

$$\begin{aligned}
|V(G)(\omega_d) - V(\bar{G})(\omega_d)| &= |\|G\|_{\omega_d}^2 - \|\bar{G}\|_{\omega_d}^2| \\
&= |\|G\|_{\omega_d} - \|\bar{G}\|_{\omega_d}| \cdot (\|G\|_{\omega_d} + \|\bar{G}\|_{\omega_d}) \\
&\le \frac{\epsilon}{\alpha}(\|G\|_{\omega_d} + \|\bar{G}\|_{\omega_d}) \\
&= \frac{\epsilon}{\alpha}(\|G\|_{\omega_d} + \|G + \bar{G} - G\|_{\omega_d}) \\
&\le \frac{\epsilon}{\alpha}(\|G\|_{\omega_d} + \|G\|_{\omega_d} + \|\bar{G} - G\|_{\omega_d}) \\
&= \frac{\epsilon}{\alpha}(2\|G\|_{\omega_d} + \|\bar{G} - G\|_{\omega_d}) \\
&\le \frac{\epsilon}{\alpha}(2\|G\|_2 + \|G - \bar{G}\|_2) \\
&\le \frac{\epsilon}{\alpha}(2\|G\|_2 + \delta) \le \frac{\epsilon}{\alpha}(2\|G\|_2 + 1) < \epsilon.
\end{aligned}$$

(The first inequality above follows from (49) and the third follows from (47).)

The second continuity statement is proved in a similar fashion. The key observation is that, for all $M \in \mathcal{RH}_\infty$ and all $\omega_d \in \mathcal{R}_+$,

$$\|M\|_{\omega_d}^2 = \frac{1}{\pi}\int_0^\infty |M(j\omega)|^2 \frac{\omega_d^2}{\omega^2+\omega_d^2}\,d\omega$$

$$\leq \frac{\|M\|_\infty^2}{\pi}\int_0^\infty \frac{\omega_d^2}{\omega^2+\omega_d^2}\,d\omega = \frac{\|M\|_\infty^2}{\pi}\left(\frac{\omega_d \pi}{2}\right) = \frac{\omega_d}{2}\|M\|_\infty^2,$$

that is,

$$\forall M \in \mathcal{RH}_\infty,\ \forall \omega_d \in \mathcal{R}_+, \quad \|M\|_{\omega_d} \leq \sqrt{\frac{\omega_d}{2}}\,\|M\|_\infty. \tag{50}$$

Combining (45) and (50) results in

$$\forall \omega_d \in \mathcal{R}_+,\ \forall \epsilon^* > 0,\ \forall G,\ \bar{G} \in \mathcal{RH}_\infty,$$

$$\left(\|G-\bar{G}\|_\infty < \sqrt{\frac{2}{\omega_d}}\epsilon^*\right) \Rightarrow (|\|G\|_{\omega_d} - \|\bar{G}\|_{\omega_d}| < \epsilon^*). \tag{51}$$

Now fix $G \in \mathcal{RH}_\infty$, $\epsilon > 0$, and $\omega_d \in \mathcal{R}_+$. Define $\alpha = \omega_d(2\|G\|_\infty + 2)/2$ and $\delta = \min(1, \epsilon/\alpha)$. Use $\epsilon^* = \sqrt{\omega_d}\epsilon/\sqrt{2}\alpha$ in (51) to obtain

$$\forall \bar{G} \in \mathcal{RH}_\infty,$$

$$\left(\|G-\bar{G}\|_\infty < \frac{\epsilon}{\alpha}\right) \Rightarrow \left(\forall \omega_d \in \mathcal{R}_+,\ |\|G\|_{\omega_d} - \|\bar{G}\|_{\omega_d}| < \sqrt{\frac{\omega_d}{2}}\,\frac{\epsilon}{\alpha}\right),$$

from which it follows that

$$\forall \bar{G} \in \mathcal{RH}_\infty,$$

$$(\|G-\bar{G}\|_\infty < \delta) \Rightarrow \left(\forall \omega_d \in \mathcal{R}_+,\ |\|G\|_{\omega_d} - \|\bar{G}\|_{\omega_d}| < \sqrt{\frac{\omega_d}{2}}\,\frac{\epsilon}{\alpha}\right). \tag{52}$$

The second continuity result follows: If $\bar{G} \in \mathcal{RH}_\infty$ satisfies $\|G - \bar{G}\|_\infty < \delta$, then

$$\begin{aligned}
|V(G)(\omega_d) - V(\bar{G})(\omega_d)| &= |\|G\|_{\omega_d}^2 - \|\bar{G}\|_{\omega_d}^2| \\
&= |\|G\|_{\omega_d} - \|\bar{G}\|_{\omega_d}| \cdot (\|G\|_{\omega_d} + \|\bar{G}\|_{\omega_d}) \\
&\le \sqrt{\frac{\omega_d}{2}} \frac{\epsilon}{\alpha} (\|G\|_{\omega_d} + \|\bar{G}\|_{\omega_d}) \\
&= \sqrt{\frac{\omega_d}{2}} \frac{\epsilon}{\alpha} (\|G\|_{\omega_d} + \|G + \bar{G} - G\|_{\omega_d}) \\
&\le \sqrt{\frac{\omega_d}{2}} \frac{\epsilon}{\alpha} (\|G\|_{\omega_d} + \|G\|_{\omega_d} + \|\bar{G} - G\|_{\omega_d}) \\
&= \sqrt{\frac{\omega_d}{2}} \frac{\epsilon}{\alpha} (2\|G\|_{\omega_d} + \|\bar{G} - G\|_{\omega_d}) \\
&\le \sqrt{\frac{\omega_d}{2}} \frac{\epsilon}{\alpha} \sqrt{\frac{\omega_d}{2}} (2\|G\|_\infty + \|G - \bar{G}\|_\infty) \\
&\le \frac{\epsilon}{\alpha} \frac{\omega_d}{2} (2\|G\|_\infty + \delta) \le \frac{\epsilon}{\alpha} \frac{\omega_d}{2} (2\|G\|_\infty + 1) < \epsilon.
\end{aligned}$$

(The first inequality follows from (52) and the third follows from (50).)

**Proof of Theorem 4.7**

The following result is used in the proof:

LEMMA *Let $f : \mathcal{R}_+ \to \mathcal{R}$ be a convex nonnegative function. Then $f^2$ is convex.*

*Proof* Let $x_1, x_2 \in \mathcal{R}_+$ and $\lambda \in [0, 1]$ be arbitrary. Since $f$ is convex,

$$f(\lambda x_1 + (1 - \lambda)x_2) \le \lambda f(x_1) + (1 - \lambda) f(x_2). \tag{53}$$

Because $f$ is nonnegative and $x^2$ is an increasing function of $x$ for $x \ge 0$, it follows that

$$f^2(\lambda x_1 + (1 - \lambda)x_2) \le [\lambda f(x_1) + (1 - \lambda) f(x_2)]^2. \tag{54}$$

Since $x^2$ is convex in $x$, it is also true that, for all $y_1, y_2 \in \mathcal{R}$,

$$[\lambda y_1 + (1 - \lambda)y_2]^2 \le \lambda y_1^2 + (1 - \lambda) y_2^2. \tag{55}$$

Evaluating (55) at $y_1 = f(x_1)$ and $y_2 = f(x_2)$ yields

$$[\lambda f(x_1) + (1-\lambda)f(x_2)]^2 \leq \lambda f^2(x_1) + (1-\lambda)f^2(x_2). \tag{56}$$

Combining (54) and (56) yields

$$f^2(\lambda x_1 + (1-\lambda)x_2) \leq \lambda f^2(x_1) + (1-\lambda)f^2(x_2), \tag{57}$$

which proves the convexity of $f^2$.

We now proceed with the proof of Theorem 4.7. Fix $\omega_d \in \mathcal{R}_+$. Define the $\|\cdot\|_{\omega_d}$ norm as in the proof of Theorem 4.6. By the triangle inequality, $\|\cdot\|_{\omega_d}$ (and, in fact, every norm) is a convex operator: $\forall G_1, G_2 \in \mathcal{RH}_\infty$, $\forall \lambda \in [0,1]$,

$$\begin{aligned}\|\lambda G_1 + (1-\lambda)G_2\|_{\omega_d} &\leq \|\lambda G_1\|_{\omega_d} + \|(1-\lambda)G_2\|_{\omega_d} \\ &= \lambda\|G_1\|_{\omega_d} + (1-\lambda)\|G_2\|_{\omega_d}.\end{aligned}$$

Since $V(G)(\omega_d) \equiv \|G\|^2_{\omega_d}$, it follows that for each $\omega_d \in \mathcal{R}_+$, $\sqrt{V(G)(\omega_d)}$ is convex in $G$. By the Lemma, it follows that for each $\omega_d \in \mathcal{R}_+$, $V(G)(\omega_d)$ is convex in $G$.

### Proof of Theorem 5.1

The following technical result, proved in [93], is needed:

LEMMA *Let $J(s) = 1/(\tau s + 1)^p$ where $p$ is a nonnegative integer and where $\tau > 0$ is a parameter. Then, for all $R \in \mathcal{RH}_2$, $\lim_{\tau \to 0}\|R(1-J)\|_2 = 0$.*

To prove the theorem, fix $\omega_d^* \in \mathcal{R}_+$. The idea of the proof of the first point in the theorem is to construct a "minimum-variance" controller, that is, a linear time-invariant (LTI) rational controller that minimizes the variance of $y$ for the particular value $\omega_d = \omega_d^*$, then to approximate that controller by a *proper* LTI rational controller. Throughout the proof, the standard acronyms ORHP (open right-half-plane), CRHP (closed right-half-plane), OLHP (open left-half-plane), and CLHP (closed left-half-plane) are used.

The minimum-variance controller development has been divided into three steps, closely following the methods used in [1]. The first step

is to use Lemma 5.2 to parameterize all internally stabilizing controllers in terms of the Youla parameter $Q$: There exist $N, M, X, Y \in \mathcal{RH}_\infty$ such that

$$P_3 P_1 = N/M \quad \text{and} \quad NX + MY = 1, \tag{58}$$

and every internally stabilizing controller $C$ can be written as

$$C = \frac{X + MQ}{Y - NQ} \tag{59}$$

for some $Q \in \mathcal{RH}_\infty$. Furthermore, every $Q \in \mathcal{RH}_\infty$ generates an internally stabilizing controller via (59).

The second step is to write $V(G)(\omega_d^*)$ in terms of $Q$. Let $\bar{F}$ denote the filter $F$ when $\omega_d = \omega_d^*$: $\bar{F}(s) = \omega_d^*/(s + \omega_d^*)$. Then,

$$\begin{aligned} G\bar{F} &= \frac{P_3 P_2 \bar{F}}{1 + P_3 P_1 C} = \frac{P_3 P_2 \bar{F}}{1 + (N/M)((X + MQ)/(Y - NQ))} \\ &= P_3 P_2 \bar{F} M Y - P_3 P_2 \bar{F} M N Q. \end{aligned} \tag{60}$$

Define

$$V = P_3 P_2 \bar{F} M Y \quad \text{and} \quad U = P_3 P_2 \bar{F} M N, \tag{61}$$

and use Lemma 5.1 to factor $U$ as $U = U_{ap} U_{mp}$. Then $G\bar{F} = V - U_{ap} U_{mp} Q$, and

$$\begin{aligned} V(G)(\omega_d^*) &= \|G\bar{F}\|_2^2 = \|V - U_{ap} U_{mp} Q\|_2^2 \\ &= \|U_{ap}(U_{ap}^{-1} V - U_{mp} Q)\|_2^2 = \|U_{ap}^{-1} V - U_{mp} Q\|_2^2, \end{aligned} \tag{62}$$

where the last equality follows because $U_{ap}$ is an all-pass filter. This completes the second step. To proceed further, the following six results are needed:

**Claim A** *$U$ and $V$ are stable.*

*Proof of Claim A* Since $P_2$, $\bar{F}$, $M$, and $N$ are stable, any unstable poles in $U = P_3 P_2 \bar{F} M N$ must be unstable poles of $P_3$. However, all CRHP poles of $P_3$ are CRHP zeros of $M$ (by (58), Lemma 5.2, and Assumption 6), so it follows that the unstable poles of $P_3$ must be canceled in

forming $P_3P_2\bar{F}MN$. Therefore, $U$ is stable. Using similar reasoning, $V = P_3P_2\bar{F}MY$ can be shown to be stable.

**Claim B** *The following set equality holds*:

$$\begin{aligned}\{\text{CRHP zeros of } U\} = {} & \{\text{CRHP zeros of } P_1\} \cup \{\text{CRHP zeros of } P_2\} \\ & \cup \{\text{CRHP zeros of } P_3\} \cup \{\text{CRHP zero of } P_3\} \\ & \cup \{\text{CRHP poles of } P_1\},\end{aligned}$$

*where set membership includes multiplicities.*

*Proof of Claim B* By Lemma 5.2, the CRHP zeros of $N$ are the CRHP zeros of $P_3P_1$ and the CRHP zeros of $M$ are the CRHP poles of $P_3P_1$. Using these facts, the fact that $\bar{F}$ has no zeros, and Assumption 6, it follows that the CRHP zeros of $U = P_3P_2\bar{F}MN$ are the members of the set

$$\begin{aligned}&\{\text{CRHP zeros of } P_3\} \cup \{\text{CRHP zeros of } P_2\} \cup \{\text{CRHP zeros of } P_3\} \\ &\quad \cup \{\text{CRHP zeros of } P_1\} \cup \{\text{CRHP poles of } P_3\} \cup \{\text{CRHP poles of } P_1\}\end{aligned}$$

that are not canceled by poles in forming $P_3P_2\bar{F}MN$. Since $P_2$, $\bar{F}$, $M$, and $N$ are stable, and since, by Claim A, $P_3P_2\bar{F}MN$ is stable, the only CRHP pole-zero cancelations are between the CRHP poles of $P_3$ and the corresponding zeros of $M$. Thus, the CRHP zeros of $U$ are

$$\begin{aligned}&\{\text{CRHP zeros of } P_3\} \cup \{\text{CRHP zeros of } P_2\} \cup \{\text{CRHP zeros of } P_3\} \\ &\quad \cup \{\text{CRHP zeros of } P_1\} \cup \{\text{CRHP poles of } P_1\}.\end{aligned}$$

**Claim C** $U_{\text{mp}}Q \in \mathcal{RH}_2$.

*Proof of Claim C* It is necessary to show that $U_{\text{mp}}Q$ is stable and strictly proper. Stability follows from the stability of $U_{\text{mp}}$ (by Claim A and Lemma 5.1) and from the stability of $Q$. Strict properness follows from the properness of $Q$, $P_3$, $P_2$, $M$, and $N$, and from the strict properness of $\bar{F}$.

**Claim D** $U_{\text{mp}}$ *has no zeros in the CRHP.*

*Proof of Claim D* By definition, $U_{\text{mp}}$ has no zeros in the ORHP, so it only remains to show that $U_{\text{mp}}$ has no zeros on the imaginary axis. Since $U_{\text{ap}}$ cannot have poles or zeros on the imaginary axis, the set of

imaginary axis zeros of $U_{mp}$ must equal the set of imaginary axis zeros of $U = U_{ap}U_{mp}$. By Claim B, this set equals the set

$$\{\text{imaginary axis zeros of } P_1\} \cup \{\text{imaginary axis zeros of } P_2\}$$
$$\cup \{\text{imaginary axis zeros of } P_3\} \cup \{\text{imaginary axis zeros of } P_3\}$$
$$\cup \{\text{imaginary axis poles of } P_1\},$$

which, by assumption, is empty.

**Claim E** $U_{ap}^{-1}V \in \mathcal{RH}_2 + \mathcal{RH}_2^{\perp}$.

*Proof of Claim E* It is necessary to show that $U_{ap}^{-1}V$ is strictly proper and that it has no poles on the imaginary axis. $U_{ap}^{-1}V$ is strictly proper since $U_{ap}$ is biproper and $V = P_3P_2\bar{F}MY$ is strictly proper. ($V$ is strictly proper since $P_3$, $P_2$, $M$, and $Y$ are proper and $\bar{F}$ is strictly proper.) $U_{ap}^{-1}V$ has no poles on the imaginary axis since $V$ is stable (by Claim A) and since $U_{ap}$ has no zeros on the imaginary axis (because $U_{ap}$ is an all-pass filter).

**Claim F** *The following set equality holds*:

$$\{\text{CRHP poles of } U_{ap}^{-1}V\}$$
$$= \{\text{ORHP zeros of } P_1\} \cup \{\text{ORHP zeros of } P_3\},$$

*where set membership includes multiplicities.*

*Proof of Claim F* By Claim E, $U_{ap}^{-1}V$ has no poles on the imaginary axis, so we need only consider ORHP poles of $U_{ap}^{-1}V$. Since $V$ is stable, any ORHP poles of $U_{ap}^{-1}V$ must also be ORHP poles of $U_{ap}^{-1}$, i.e., ORHP zeros of $U_{ap}$. Such zeros coincide with the ORHP zeros of $U$. Therefore, the ORHP poles of $U_{ap}^{-1}V$ are the ORHP zeros of $U = P_3P_2\bar{F}MN$ that are not also ORHP zeros of $V = P_3P_2\bar{F}MY$. These are exactly the ORHP zeros of $N$ that are not also ORHP zeros of $Y$. But $N$ and $Y$ have no common ORHP zeros: If they did, say at $s = s_0$, then, by the stability of $X$ and $M$, $N(s_0)X(s_0) + M(s_0)Y(s_0) = 0$, which contradicts (58). Therefore, the ORHP poles of $U_{ap}^{-1}V$ are the ORHP zeros of $N = P_3P_1$. The proof is complete on recognition that the ORHP zeros of $P_3P_1$ are $\{\text{ORHP zeros of } P_1\} \cup \{\text{ORHP zeros of } P_3\}$, by Assumption 6.

The third step in the minimum-variance control development is to find the stable transfer function $Q$ that minimizes (62). Use Claim E and Lemma 5.3 to write $U_{ap}^{-1}V = (U_{ap}^{-1}V)_{st} + (U_{ap}^{-1}V)_{un}$. Hence, by (62),

$$V(G)(\omega_d^*) = \|(U_{ap}^{-1}V)_{st} + (U_{ap}^{-1}V)_{un} - U_{mp}Q\|_2^2. \tag{63}$$

By Claim C, the second part of Lemma 5.3 can be applied to (63) to yield

$$V(G)(\omega_d^*) = \|(U_{ap}^{-1}V)_{un}\|_2^2 + \|(U_{ap}^{-1}V)_{st} - U_{mp}Q\|_2^2. \tag{64}$$

By Claim D, $U_{mp}^{-1}$ is stable, so if $Q$ is chosen to be the stable (but possibly improper) transfer function

$$Q_{im} \triangleq U_{mp}^{-1}(U_{ap}^{-1}V)_{st}, \tag{65}$$

then (64) is minimized, and the minimum variance is

$$\|(U_{ap}^{-1}V)_{un}\|_2^2. \tag{66}$$

If $Q_{im}$ happens to be proper, then the minimum-variance controller development is complete: use $Q = Q_{im}$ in (59) to compute the controller. On the other hand, if $Q_{im}$ is improper, then it is necessary to find a proper $Q$ that is "close" to the optimal $Q_{im}$; an appropriate choice for $Q$ is

$$Q(s) = Q_{im}(s)\frac{1}{(\tau s + 1)^p}, \tag{67}$$

where $p > 0$ is an integer sufficiently large so that $Q$ is proper, and where $\tau > 0$ is a small real number. This is an "appropriate" choice for $Q$ since the variance (64) converges to (66) as $\tau \to 0$. (To prove this, let $J(s) = 1/(\tau s + 1)^p$ and $R = (U_{ap}^{-1}V)_{st}$. Then the difference between (64) and (66) is $\|R(1 - J)\|_2^2$, which, by the Lemma at the beginning of the proof, tends to zero as $\tau \to 0$.)

We now invoke the minimum-phase assumption (i.e., the third assumption in the theorem statement). Since the zeros of $P_1$ and $P_3$ are in the OLHP, it follows from Claim F that $U_{ap}^{-1}V$ is stable. Hence, $(U_{ap}^{-1}V)_{un} = 0$ and $(U_{ap}^{-1}V)_{st} = U_{ap}^{-1}V$. Thus, in the minimum-phase case, the minimum variance (66) is zero, and the optimal $Q_{im}$,

from (65), is

$$Q_{\text{im}} = U_{\text{mp}}^{-1}(U_{\text{ap}}^{-1}V)_{\text{st}} = U_{\text{mp}}^{-1}U_{\text{ap}}^{-1}V = \frac{V}{U} = \frac{P_3P_2\bar{F}MY}{P_3P_2\bar{F}MN} = \frac{Y}{N}.$$

Hence, the Youla parameter for the minimum-phase case is

$$Q(s) = \frac{Y(s)}{N(s)}\frac{1}{(\tau s+1)^p}, \tag{68}$$

where $p \geq 0$ is a sufficiently large integer and where $\tau > 0$ is a parameter. Given $\epsilon > 0$, the closed-loop variance can be made less than $\epsilon$ by choosing sufficiently small $\tau$. This proves the first point in the theorem.

To prove the second point in the theorem, note that, since $\Omega$ is bounded, there exists a $\omega_{\text{d}}^* \in \mathcal{R}_+$ such that $\omega_{\text{d}} \in \Omega \Rightarrow \omega_{\text{d}} < \omega_{\text{d}}^*$. Using this value of $\omega_{\text{d}}^*$ in (28) yields

$$\forall \epsilon > 0, \ \exists \bar{\tau} > 0 \text{ such that } \forall \tau \in (0, \bar{\tau}), \quad V(G)(\omega_{\text{d}}^*) < \epsilon.$$

This, together with the fact that $V$-transforms are increasing functions (Theorem 4.3), proves the second point.

To prove the third point, fix $\omega_{\text{d}}^* > 0$ and $\gamma > 0$. By definition of $\text{DGM}_\gamma$, for sufficiently small $V(G)(\omega_{\text{d}}^*)$, $\text{DGM}_\gamma$ can be made arbitrarily large. Hence, by (28), there exists a $\bar{\tau}$ (call it $\bar{\tau}_1$) such that $\forall \tau \in (0, \bar{\tau}_1)$, $\text{DGM}_\gamma \geq \text{DGM}_{\text{min}}$. Similarly, there exists a $\bar{\tau}_2$ such that $\forall \tau \in (0, \bar{\tau}_2)$, $\text{DBM}_\gamma \geq \text{DBM}_{\text{min}}$. Choose $\bar{\tau} = \min\{\bar{\tau}_1, \bar{\tau}_2\}$ to complete the proof.

### Proof of Theorem 5.2

The proof proceeds exactly as the proof of Theorem 5.1 up to the end of the paragraph that includes Eq. (67). The expression in (66) plays the role of $\alpha$ in the theorem statement; it is nonzero if and only if $U_{\text{ap}}^{-1}V$ has ORHP poles, which, by Claim F, occurs precisely when either $P_1$ or $P_3$ has ORHP zeros. The Youla parameter in (30) is that in (67). Property (31) follows by the discussion immediately following (67).

To prove the second point in the theorem, define $B_{\text{min}} : \mathcal{R}_+ \to \mathcal{R}_+$ as follows: $B_{\text{min}}(0) = 0$, and, for all $\omega_{\text{d}} > 0$, $B_{\text{min}}(\omega_{\text{d}}) = \alpha$, where $\alpha$ is the $\alpha$ from the first point in the theorem evaluated at $\omega_{\text{d}}^* = \omega_{\text{d}}$. It follows immediately that $B_{\text{min}}$ is a lower bound of the $V$-transform of any

internally-stabilizing controller, achievable by the controller with Youla parameter (30) in the limit $\tau \to 0$. The fact that $B_{\min}(\omega_d)$ is the infimum of achievable variances at $\omega_d$ and the fact that $V$-transforms are strictly increasing functions imply that $B_{\min}$ is a strictly increasing function. The fact that $B_{\min}$ is an analytic function follows because $U_{ap}^{-1}V$, and, hence, $\|(U_{ap}^{-1}V)_{un}\|_2^2$, is rational in $\omega_d^*$.

The third part of the theorem follows immediately from the definition of $\mathrm{DGM}_\gamma$ and the selection of $B_{\min}$: For fixed $\omega_d^* > 0$ and $\gamma > 0$, set

$$\mathrm{DGM}_{\max} = \sqrt{\frac{\gamma}{B_{\min}(\omega_d^*)}}.$$

To prove the final point, fix $\omega_d^* > 0$. Then note that $B_{\min}$ being nonzero implies that there exists a $\bar{\gamma} > 0$ and a scalar $\mathrm{DBM}_{\max}$ such that for all internally stabilizing controllers $\mathrm{DBM}_{\bar{\gamma}} \leq \mathrm{DBM}_{\max}$; in particular, choose $\bar{\gamma}$ to be any nonzero value in the range of function $B_{\min}$, and then set $\mathrm{DBM}_{\max} = \bar{\omega}_b/\omega_d^*$, where $\bar{\omega}_b > 0$ satisfies $B_{\min}(\bar{\omega}_b) = \bar{\gamma}$. The desired result then follows because $B_{\min}$ is an increasing function.

**Proof of Theorem 5.3**

The idea behind the proof is simply to compute $\alpha$ from Theorem 5.2. First consider the case where the nonminimum-phase zero is in $P_3$. Define, in addition to $\bar{P}_3$ and $\bar{M}$,

$$\bar{N}(s) = \frac{N(s)}{s-z} \quad \text{and} \quad \bar{P}_1(s) = \left[\prod_{i=1}^{n_1}(s-p_{1,i})\right] P_1(s).$$

From Theorem 5.2, we then have

$$U = (s-z)^2\left[\prod_{i=1}^{n_1}(s-p_{1,i})\right]\bar{P}_3 P_2 F^* \bar{M}\bar{N},$$

$$V = (s-z)\left[\prod_{i=1}^{n_1}(s-p_{1,i})\right]\bar{P}_3 P_2 F^* \bar{M} Y.$$

Therefore,

$$U_{ap} = \frac{(s-z)^2[\Pi_{i=1}^{n_1}(s-p_{1,i})]}{(s+z)^2[\Pi_{i=1}^{n_1}(s+p_{1,i})]}$$

and

$$U_{\text{ap}}^{-1}V = \frac{(s+z)^2[\Pi_{i=1}^{n_1}(s+p_{1,i})]}{(s-z)}\bar{P}_3P_2F^*\bar{M}Y = \frac{A}{s-z} + B,$$

where $B$ is a stable transfer function and $A$ is the residue

$$A = 4z^2\left[\prod_{i=1}^{n_1}(z+p_{1,i})\right]\bar{P}_3(z)P_2(z)F^*(z)\bar{M}(z)Y(z).$$

Thus,

$$(U_{\text{ap}}^{-1}V)_{\text{un}} = \frac{A}{s-z}.$$

Because there are no unstable pole-zero cancelations in $P_1P_3$ (by Assumption 6) and neither $P_1$ nor $P_3$ has zeros on the imaginary axis (by assumption in the theorem statement), it follows from Theorem 5.2 that the minimum achievable variance is

$$\begin{aligned}\alpha &= \left\|\frac{A}{s-z}\right\|_2^2 = \frac{A^2}{2z} \\ &= 8z^3\left[\prod_{i=1}^{n_1}(z+p_{1,i})^2\right]\bar{P}_3^2(z)P_2^2(z)[F^*(z)]^2\bar{M}^2(z)Y^2(z),\end{aligned}$$

which is the desired result. The case where the nonminimum-phase zero is in $P_1$ is similar.

### Acknowledgments

This research was supported by the Army Research Office under Grant DAAL03-92-G-0127. The first author would also like to acknowledge funding from the Natural Sciences and Engineering Research Council of Canada.

### References

[1] J.C. Doyle, B.A. Francis and A.R. Tannenbaum, *Feedback Control Theory*, Macmillan, New York, NY, 1992.

[2] M. Morari and E. Zafiriou, *Robust Process Control*, Prentice-Hall, Englewood Cliffs, NJ, 1989.

[3] M. Green and D.J.N. Limebeer, *Linear Robust Control*, Prentice-Hall, Englewood Cliffs, NJ, 1995.

[4] P. Dorato, R. Tempo and G. Muscato, Bibliography on robust control, *Automatica – J. IFAC* **29**(1) (1993) 201–213.
[5] K. Zhou, J.C. Doyle and K. Glover, *Robust and Optimal Control*, Prentice-Hall, Upper Saddle River, NJ, 1996.
[6] National Transportation Safety Board, Incident Identification NYC97LA040, Washington, DC, 20594, January 1997 (also see http://www.ntsb.gov/Aviation/9701.htm).
[7] B. Etkin, Turbulent wind and its effect on flight, *AIAA J. Aircraft* **18**(5) (1981) 327–345.
[8] J. Roskam, *Airplane Design Part VII: Determination of Stability, Control and Performance Characteristics – FAR and Military Requirements*, Roskam Aviation and Engineering Corporation, Route 4, Box 274, Ottawa, Kansas, 66067, 1985.
[9] D. Hrovat, Applications of optimal control to advanced automotive suspension design, *Trans. ASME J. Dynamic Systems Meas. Control* **115**(2(B)) (1993) 328–342.
[10] A. Hać, Adaptive control of vehicle suspension, *Vehicle System Dynamics* **16**(2) (1987) 57–74.
[11] W.R. Hudson, D. Halbach, J.P. Zaniewski and L. Moser, Root-mean-square vertical acceleration as a summary roughness statistic, *Measuring Road Roughness and its Effects on User Cost and Comfort* (Philadelphia) (T.D. Gillespie and M. Sayers, Eds.), ASTM, 1985, pp. 3–24.
[12] C.C. Smith, D.Y. McGehee and A.J. Healey, The prediction of passenger riding comfort from acceleration data, *Trans. ASME J. Dynamic Systems Meas. Control* **100** (1978) 34–41.
[13] S.M. Meerkov and T. Runolfsson, Residence time control, *IEEE Trans. Automat. Control* **33**(4) (1988) 323–332.
[14] S.M. Meerkov and T. Runolfsson, Output residence time control, *IEEE Trans. Automat. Control* **34**(11) (1989) 1171–1176.
[15] S. Kim, S.M. Meerkov and T. Runolfsson, Residence probability control, *Computers Math. with App.* **19**(11) (1990) 121–125.
[16] S. Kim, S.M. Meerkov and T. Runolfsson, Aiming control: Residence probability and $(D, T)$-stability, *Automatica – J. IFAC* **28**(3) (1992) 549–555.
[17] S.M. Meerkov and T. Runolfsson, Theory of residence-time control by output feedback, *Dynamics Control* **1** (1991), 63–81.
[18] S. Kim, S.M. Meerkov and T. Runolfsson, Aiming control: Design of residence probability controllers, *Automatica – J. IFAC* **28**(3) (1992), 557–564.
[19] D. McRuer, I. Ashkenas and D. Graham, *Aircraft Dynamics and Automatic Control*, Princeton University Press, Princeton, New Jersey, 1973.
[20] F.M. Hoblit, *Gust Loads on Aircraft: Concepts and Applications*, AIAA Education Series, American Institute of Aeronautics and Astronautics, Washington, DC, 1988.
[21] W.G. Price and R.E.D. Bishop, *Probabilistic Theory of Ship Dynamics*, John Wiley & Sons, New York, 1974.
[22] H. Stark and J.W. Woods, *Probability, Random Processes, and Estimation Theory for Engineers*, 2nd ed., Prentice-Hall, Englewood Cliffs, NJ, 1994.
[23] B. Etkin and L.D. Reid, *Dynamics of Flight: Stability and Control*, 3rd ed., John Wiley & Sons, New York, 1996.
[24] J. Roskam, *Airplane Flight dynamics and Automatic Flight Controls: Part II*, Roskam Aviation and Engineering Corp., Kansas City, 1979.
[25] G.H. Gaonkar, Gust response of rotor and propellor systems, *AIAA J. Aircraft* **18**(5) (1981) 389–396.
[26] C.R. Chalk, T.P. Neal, T.M. Harris, F.E. Pritchard and J.J. Woodcock, Background information and user guide for MIL F-8785B (ASG), entitled military specification – Flying qualitites of piloted airplanes, Tech. Report AFFDL TR-69-72, Air Force Flight Dynamics Laboratory, Dayton, OH, August 1969.
[27] J.C. Houbolt, Atmospheric turbulence, *AIAA J.* **11**(4) (1973) 421–437.
[28] M. Labarrère and Y. Negre, Wing load alleviation modelling, *Systems and Control Encyclopedia: Theory, Technology, Applications*, Pergamon Press, 1987, pp. 5164–5170.

[29] A.R.J.M. Lloyd, *Seakeeping: Ship Behaviour in Rough Weather*, John Wiley & Sons, New York, 1989.
[30] G. Neumann and W.J. Pierson, Jr., *Principles of Physical Oceanography*, Prentice-Hall, Englewoods Cliffs, NJ, 1966.
[31] B. Kinsman, *Wind Waves: Their Generation and Propagation on the Ocean Surface*, Prentice-Hall, Englewoods Cliffs, NJ, 1965.
[32] H.U. Sverdrup and W.H. Munk, Wind, sea, and swell: Theory of relations for forecasting, Tech. Report 601, US Navy Hydrographic Office, Washington, DC, March 1947.
[33] J.B. Herbich (Ed.), *Handbook of Coastal and Ocean Engineering*, Vol. 1, Gulf Publishing, Houston, TX, 1990.
[34] R.E.D. Bishop and W.G. Price, *Hydroelasticity of Ships*, Combridge University Press, London, 1979.
[35] J.P. Comstock (Ed.), *Principles of Naval Architecture*, The Society of Naval Architects and Marine Engineers, New York, 1967.
[36] *Ocean Wave Spectra*, Prentice-Hall, Englewoods Cliffs, NJ, May 1961.
[37] M. Sayers, Development, implemenation, and applications of the reference quarter-car simulation, *Measuring Road Roughness and its Effects on User Cost and Comfort* (Philadelphia) (T.D. Gillespie and M. Sayers, Eds.), ASTM, 1985, pp. 25–47.
[38] W.D.O. Paterson, Accuracy of calibrated roughness surveys, *Measuring Road Roughness and its Effects on User Cost and Comfort* (Philadelphia) (T.D. Gillespie and M. Sayers, Eds.), ASTM, 1985, pp. 66–88.
[39] J.P. Zaniewski and B.C. Butler, Vehicle operating costs related to operating mode, road design, and pavement condition, *Measuring Road Roughness and its Effects on User Cost and Comfort* (Philadelphia) (T.D. Gillespie and M. Sayers, Eds.), ASTM, 1985, pp. 127–142.
[40] A.J. Healey, E. Nathman and C.C. Smith, An analytical and experimental study of automobile dynamics with random roadway inputs, *Trans. ASME J. Dynamic Systems Meas. Control* **99**(4(G)) (1977) 284–292.
[41] C.J. Dodds and J.D. Robson, The description of road surface roughness, *J. Sound Vibration* **31**(2) (1973) 175–183.
[42] V. Bormann, Messungen von Fahrbahn-Unebenheiten paralleler Fahrspuren und Anwendung der Ergebnisse, *Vehicle System Dynamics* **7**(2) (1978) 65–81, (in German).
[43] X.-P. Lu, Effects of road roughness on vehicular rolling resistance, *Measuring Road Roughness and its Effects on User Cost and Comfort* (Philadelphia) (T.D. Gillespie and M. Sayers, Eds.), ASTM, 1985, pp. 143–161.
[44] T. Dahlberg, An optimized speed-controlled suspension of a 2-DOF vehicle travelling on a randomly profiled road, *J. Sound Vibration* **62**(4) (1979) 541–546.
[45] A. Hać, Suspension optimization of a 2-DOF vehicle model using a stochastic optimal control technique, *J. Sound Vibration* **100**(3) (1985) 343–357.
[46] W.A. Stauffer and F.M. Hoblit, Dynamic gust, landing, and taxi loads determinations in the design of the L-1011, *AIAA J. Aircraft* **10**(8) (1973) 459–467.
[47] J.K. Hedrick, G.F. Billington and D.A. Dreesbach, Analysis, design, and optimization of high speed vehicle suspensions using state variable techniques, *Trans. ASME J. Dynamic Systems Meas. Control* **96**(2(G)) (1974) 193–203.
[48] M. Nagai and M. Iguchi, Vibrational characteristics of electromagnetic levitation vehicles-guideway systems, *Vehicle System Dynamics* **8**(2) (1979) 177–181 (extended abstract).
[49] S.P. Boyd and C.H. Barratt, *Linear Controller Design: Limits of Performance*, Prentice-Hall, Englewood Cliffs, NJ, 1991.
[50] E. Liceaga-Castro and G.M. van der Molen, Submarine $H^{\infty}$ Depth control under wave disturbances, *IEEE Trans. Control Systems Tech.* **3**(3) (1995) 338–346.
[51] A. Francescutto, On the nonlinear motions of ships and structures in narrow band sea, *Dynamics of Marine Vehicles and Structures in Waves* (W.G. Price, P. Temarel

and A.J. Keane, Eds.), Developments in Marine Technology, No. 7, Elsevier, Amsterdam, UK, June 1991, pp. 291–303.
[52] V. Poor and D.P. Looze, Minimax state estimation for linear stochastic systems with noise uncertainty, *IEEE Trans. Automat. Control* **AC-26**(4) (1981) 902–906.
[53] S.A. Kassam, T.L. Lim and L.J. Cimini, Two-dimensional filters for singal processing under modeling uncertainties, *IEEE Trans. Geosci. Remote Sensing* **GE-18**(4) (1980) 331–336.
[54] H.V. Poor, On robust Wiener filtering, *IEEE Trans. Automat. Control* **AC-25**(3) (1980) 531–536.
[55] M.C. Yovits and J.L. Jackson, Linear filter optimization with game theory considerations, *IRE National Convention Record* **4** (1955) 193–199.
[56] J.M. Morris, The Kalman filter: A robust estimator for some classes of linear quadratic problems, *IEEE Trans. Inform. Theory* **IT-22**(5) (1976) 526–534.
[57] D.P. Looze, H.V. Poor, K.S. Vastola and J.C. Darragh, Minimax control of linear stochastic systems with noise uncertainty, *IEEE Trans. Automat. Control* **AC-28**(9) (1983) 882–888.
[58] B.-S. Chen and T.-Y. Dong, LQG optimal control system design under plant perturbation and noise uncertainty: A state-space approach, *Automatica – J. IFAC* **25**(3) (1989) 431–436.
[59] S.-H. Chen, J.-H. Chou and C.-H. Chao, Stability robustness of the LQG system with noise uncertainty and nonlinear/linear time-varying plant perturbations, *JSME Internat. J. Ser. C* **39**(1) (1996) 67–72.
[60] J.S. Luo and A. Johnson, Stability robustness of the continuous-time LQG system under plant perturbation and noise uncertainty, *Automatica – J. IFAC* **29**(2) (1993) 485–489.
[61] S.V. Gusev, Minimax control under a bound on the partial covariance sequence of the disturbance, *Automatica – J. IFAC* **31**(9) (1995) 1287–1301.
[62] S.V. Gusev, Minimax control under a restriction of the moments of disturbance, *Proc. 34th Conf. Decision and Control* (New Orleans, LA), IEEE, December 1995, pp. 1195–1200.
[63] S.V. Gusev, Minimax control for linear discrete-time systems, *Proc. Third European Control Conf. ECC 95* (Rome) (A. Isidori, S. Bittanti, E. Mosca, A. De Luca, M.D. Di Benedetto and G. Oriolo, Eds.), Vol. 3, EUCA, September 1995, pp. 2591–2596.
[64] S.V. Gusev, Method of moment restrictions in robust control and filtering, *IFAC World Congress* (San Francisco), IFAC, July 1996.
[65] N.E. Hahi and I.M. Weiss, Optimum Wiener bounding filters in the presence of uncertainties, *Inform. and Control* **28**(3) (1975) 179–191.
[66] T.L. Greenlee and C.T. Leondes, Generalized bounding filters for linear time invariant systems, *Decision and Control Conf.* (New Orleans, LA), IEEE, December 1977, pp. 585–590.
[67] N.E. Hahi and I.M. Weiss, Bounding filter: A simple solution to Loack of exact a priori statistics, *Inform. and Control* **39**(2) (1978) 212–224.
[68] V.A. Yakubovich, Optimal damping of forced stochastic oscillations in linear systems in the case of unknown spectral density of external disturbance, *Proc. 35th Conf. on Decision and Control* (Kobe, Japan), IEEE, December 1996, pp. 3200–3203.
[69] G. Zames, Feedback and optimal sensitivity: Model reference transformations, multiplicative seminorms, and approximate inverses, *IEEE Trans. Automat. Control* **AC-26**(2) (1981) 301–320.
[70] G. Zames and B.A. Francis, Feedback, minimax sensitivity, and optimal robustness, *IEEE Trans. Automat. Control* **AC-28**(5) (1983) 585–601.
[71] J.A. Tenney and M. Tomizuka, Effects of non-periodic disturbances on repetitive control systems, *13th Triennial World Congress* (San Francisco, CA), Vol. 2A-14 2, IFAC, July 1996, pp. 7–12.
[72] E.W. Kamen and P.P. Khargonekar, On the control of linear systems whose coefficients are functions of parameters, *IEEE Trans. Automat. Control* **AC-29**(1) (1984) 25–33.

[73] K.J. Åström and B. Wittenmark, *Adaptive Control*, 2nd ed., Addison Wesley, New York, NY, 1995.
[74] S. Verdú and V. Poor, Minimax linear observers and regulators for stochastic systems with uncertain second-order statistics, *IEEE Trans. Automat. Control* **AC-29**(6) (1984) 499–511.
[75] J.C. Doyle, K. Glover, P.P. Khargonekar and B.A. Francis, State-space solutions to standard $\mathcal{H}_2$ and $\mathcal{H}_\infty$ control problems, *IEEE Trans. Automat. Control* **34**(8) (1989) 831–847.
[76] The Mathworks Inc., 24 Prime Park Way, Natick, MA, 01760, *Robust Control Toolbox*, August 1992.
[77] M.J. Grimble, LQG Optimal control design for uncertain systems, *IEE Proc.-D* **139**(1) (1992) 21–30.
[78] L.R. Ray, Robust linear-optimal control laws for active suspension systems, *The Winter Annual Meeting of the ASME: Advanced Automotive Technologies 1991*, Atlanta, GA, December 1991, pp. 291–302.
[79] P.H. McDowell and T. Basar, Robust controller design for linear stochastic systems with uncertain parameters, *1986 American Control Conf.* (Seattle, WA), Vol. 1, IEEE, June 1986, pp. 39–44.
[80] X.Y. Gu and W.H. Chen, Design of suboptimal minimax LQG controller via game theory, *American Control Conf.* (Boston, MA), Vol. 1, June 1991, pp. 376–377.
[81] D.S. Bernstein and S.W. Greeley, Robust controller synthesis using the maximum entropy design equations, *IEEE Trans. Automat. Control* **AC-31**(4) (1986) 362–364.
[82] M. Tahk and J.L. Speyer, Modeling of parameter variations and asymptotic LQG synthesis, *Proc. 25th Conf. Decision and Control* (Athens, Greece), Vol. 3, IEEE, December 1986, pp. 1459–1465.
[83] M. Tahk and J.L. Speyer, A parameter robust LQG design synthesis with applications to control of flexible structures, *1987 American Control Conf.* (Minneapolis, MN), Vol. 1, IEEE, June 1987, pp. 386–392.
[84] S.S.L. Chang and T.K.C. Peng, Adaptive guaranteed cost control of systems with uncertain parameters, *IEEE Trans. Automat. Control* **AC-17**(4) (1972) 474–483.
[85] C.T. Liou and C.T. Yang, Guaranteed cost control of tracking problems with large plant uncertainty, *Internat. J. Control* **45**(6) (1987) 2161–2171.
[86] I.R. Peterson and D.C. McFarlane, Optimal guaranteed cost control and filtering for uncertain linear systems, *IEEE Trans. Automat. Control* **39**(9) (1994) 1971–1977.
[87] J.H. Friedman, P.T. Kabamba and P.P. Khargonekar, Worst-case and average $\mathcal{H}_2$ performance analysis against real constant parametric uncertainty, *Automatica – J. IFAC* **31**(4) (1995) 649–657.
[88] E.J. Davison and B. Scherzinger, Perfect control of the robust servomechanism problem, *IEEE Trans. Automat. Control* **32**(8) (1987) 689–702.
[89] L. Qiu and E.J. Davison, Performance limitations of non-minimum phase systems in the servomechanism problem, *Automatica – J. IFAC* **29**(2) (1993) 337–349.
[90] D.E. Davison, P.T. Kabamba and S.M. Meerkov, Disturbance gain and bandwidth margins: Definitions and application to autopilot design, *American Control Conf.* (Albuquerque, NM), IEEE, June 1997.
[91] F.L. Lewis, *Optimal Control*, John Wiley & Sons, New York, 1986.
[92] W. Fulks, *Advanced Calculus: An Introduction to Analysis*, 3rd ed., John Wiley & Sons, New York, NY, 1978.
[93] B.A. Francis, On the Wiener–Hopf approach to optimal feedback design, *Systems Control Lett.* **2** (1982) 197–201.

Mathematical Problems in Engineering

# Special Issue on Space Dynamics

## Call for Papers

Space dynamics is a very general title that can accommodate a long list of activities. This kind of research started with the study of the motion of the stars and the planets back to the origin of astronomy, and nowadays it has a large list of topics. It is possible to make a division in two main categories: astronomy and astrodynamics. By astronomy, we can relate topics that deal with the motion of the planets, natural satellites, comets, and so forth. Many important topics of research nowadays are related to those subjects. By astrodynamics, we mean topics related to spaceflight dynamics.

It means topics where a satellite, a rocket, or any kind of man-made object is travelling in space governed by the gravitational forces of celestial bodies and/or forces generated by propulsion systems that are available in those objects. Many topics are related to orbit determination, propagation, and orbital maneuvers related to those spacecrafts. Several other topics that are related to this subject are numerical methods, nonlinear dynamics, chaos, and control.

The main objective of this Special Issue is to publish topics that are under study in one of those lines. The idea is to get the most recent researches and published them in a very short time, so we can give a step in order to help scientists and engineers that work in this field to be aware of actual research. All the published papers have to be peer reviewed, but in a fast and accurate way so that the topics are not outdated by the large speed that the information flows nowadays.

Before submission authors should carefully read over the journal's Author Guidelines, which are located at http://www.hindawi.com/journals/mpe/guidelines.html. Prospective authors should submit an electronic copy of their complete manuscript through the journal Manuscript Tracking System at http://mts.hindawi.com/ according to the following timetable:

| | |
|---|---|
| Manuscript Due | July 1, 2009 |
| First Round of Reviews | October 1, 2009 |
| Publication Date | January 1, 2010 |

**Lead Guest Editor**

**Antonio F. Bertachini A. Prado,** Instituto Nacional de Pesquisas Espaciais (INPE), São José dos Campos, 12227-010 São Paulo, Brazil; prado@dem.inpe.br

**Guest Editors**

**Maria Cecilia Zanardi,** São Paulo State University (UNESP), Guaratinguetá, 12516-410 São Paulo, Brazil; cecilia@feg.unesp.br

**Tadashi Yokoyama,** Universidade Estadual Paulista (UNESP), Rio Claro, 13506-900 São Paulo, Brazil; tadashi@rc.unesp.br

**Silvia Maria Giuliatti Winter,** São Paulo State University (UNESP), Guaratinguetá, 12516-410 São Paulo, Brazil; silvia@feg.unesp.br